AD NUMBER
ADC003503
CLASSIFICATION CHANGES
TO: unclassified
FROM: secret
LIMITATION CHANGES
TO: Approved for public release, distribution unlimited
FROM: Distribution authorized to U.S. Gov't. agencies only; Foreign Government Information; 01 FEB 1974. Other requests shall be referred to Commander, Air force Systems Command, Attn: SDE, Washington, DC 20334.
AUTHORITY
31 Dec 1984, per document marking; NRL Code/5309 memo dtd 20 Feb 1997

NRL Memorandum Report 2722
Copy No. 22

ESD-TR-73-270, Vol. II, Pt G

SECRET

AN/FPS-95 RESEARCH AND DEVELOPMENT PROGRAM (FINAL TECHNICAL REPORT, NAVAL RESEARCH LABORATORY, PERFORMANCE PREDICTION EFFECTS) (U)

J. M. Hudnall
Naval Research Laboratory
Washington, D. C. 20375

March 1974

Distribution limited to U.S. Gov't agencies only; Foreign Information; 1 February 1974. Other requests for this document must be referred to Hq AFSC (SDE).

NATIONAL SECURITY INFORMATION
Unauthorized Disclosure Subject to Criminal Sanctions

Classified by ESD/OC
Exempt from General Declassification Schedule of Executive Order 11652
Exemption Category: 3
Declassify on: 31 December 1984

Prepared for

DEPUTY FOR SURVEILLANCE AND CONTROL SYSTEMS
HQ ELECTRONIC SYSTEMS DIVISION (AFSC)
L. G. Hanscom Field, Bedford, MA 01730

LEGAL NOTICE

When U. S. Government drawings, specifications or other data are used for any purpose other than a definitely related government procurement operation, the government thereby incurs no responsibility nor any obligation whatsoever; and the fact that the government may have formulated, furnished, or in any way supplied the said drawings, specifications, or other data is not to be regarded by implication or otherwise as in any manner licensing the holder or any other person or conveying any rights or permission to manufacture, use, or sell any patented invention that may in any way be related thereto.

OTHER NOTICES

Do not return this copy. Retain or destroy, in accordance with pertinent Security Regulations.

This technical report has been reviewed and is approved for publication.

JAMES M. HEADRICK, Branch Head
Radar Techniques Branch
Radar Division, Naval Research Laboratory

RICHARD W. CORAINE, Lt Col, USAF
Chief, 441 A
Engineering Division

FOR THE COMMANDER

DONALD W. LAMBRECHT, Colonel, USAF
System Program Director

SECRET

(This Page is Unclassified)

(18) ESD

SECRET (19) TR-73-270-Vol-2-Pt-G

SECURITY CLASSIFICATION OF THIS PAGE (When Data Entered)

REPORT DOCUMENTATION PAGE	READ INSTRUCTIONS BEFORE COMPLETING FORM
1. REPORT NUMBER (14) NRL-MR- NRL Memorandum Report 2722	2. GOVT ACCESSION NO. (4) 3. RECIPIENT'S CATALOG NUMBER Rept for 1971-1973
4. TITLE (and Subtitle) (6) AN/FPS-95 RESEARCH AND DEVELOPMENT PROGRAM (FINAL TECHNICAL REPORT, NAVAL RESEARCH LABORATORY, PERFORMANCE PREDICTION EFFECTS) (U) (8)	5. TYPE OF REPORT & PERIOD COVERED Final report covering period 1971-1973
	6. PERFORMING ORG. REPORT NUMBER
7. AUTHOR(s) (10) James M. Hudnall	8. CONTRACT OR GRANT NUMBER(s) ~~USAF-MIPR-FY76207300001~~
9. PERFORMING ORGANIZATION NAME AND ADDRESS Naval Research Laboratory Washington, D. C. 20375	10. PROGRAM ELEMENT, PROJECT, TASK AREA & WORK UNIT NUMBERS (16) NRL [redacted] R02-42
11. CONTROLLING OFFICE NAME AND ADDRESS Deputy for Surveillance and Control Systems Hq Electronic Systems Division, L. G. Hanscom Fld, MA	12. REPORT DATE March 1974
	13. NUMBER OF PAGES 58 (12) 55p.
14. MONITORING AGENCY NAME & ADDRESS (if different from Controlling Office) Hq AFSC (SDE) Andrews AFB, Washington, D. C. 20334	15. SECURITY CLASS. (of this report) SECRET
	15a. DECLASSIFICATION/DOWNGRADING SCHEDULE Exempt-Exemp Cat: 3

16. DISTRIBUTION STATEMENT (of this Report)

Distribution limited to U. S. Gov't agencies only; Foreign Information; 1 February 1974. Other requests for this document must be referred to Hq AFSC (SDE).

DDC RETURNED OCT 15 1975 D

17. DISTRIBUTION STATEMENT (of the abstract entered in Block 20, if different from Report)

18. SUPPLEMENTARY NOTES

19. KEY WORDS (Continue on reverse side if necessary and identify by block number)

HF radar
Radar management
Frequency diversity

20. ABSTRACT (Continue on reverse side if necessary and identify by block number) (SECRET)

A comparison between predicted signal returns on the AN/FPS-95 and the observed signal returns from switched reflectors was made. Included in this report are amplitude-time records of both the ground backscatter and the reflector signals. An example is shown which illustrates how frequency diversity improves the detection of the reflector.

DD FORM 1 JAN 73 1473 EDITION OF 1 NOV 65 IS OBSOLETE S/N 0102-014-6601 | i SECRET

SECURITY CLASSIFICATION OF THIS PAGE (When Data Entered)

251 950

TABLE OF CONTENTS

SECRET

FINAL TECHNICAL REPORT ON THE AN/FPS-95 RESEARCH AND DEVELOPMENT PROGRAM VOL. II, PART G. PERFORMANCE PREDICTION EFFECTS (U)

I. INTRODUCTION (U)

(S) As a part of the overall program of evaluating performance of the AN/FPS-95 Radar Set, radar data have been collected for the four switched reflectors installed in the radar's coverage. The purpose of this paper is to describe the data collected and to compare it with the median predictions generated for the month.

II. COMPUTATION OF EXPECTED SIGNAL STRENGTH (U)

(U) The received power expected from a target can be calculated by the radar equation. A basic form of the radar equation is:

$$P_r = P_t \frac{G^2 \lambda^2 \sigma}{(4\pi)^3 R^4 L_p L_s} \qquad (1)$$

where

P_r = received power

P_t = transmitted power

G = antenna gain

λ = wave length

σ = target radar cross section

R = target slant range

L_p = propagation losses

L_s = system hardware losses

The equation can be rewritten in a logarithmic form as

$$P_r = P_t + G + \sigma - 40\log R - 20\log F - 84.15 - L_p - L_s \qquad (2)$$

where

P_r = received power (dBm)

P_t = transmitted power (dBW)

G = two-way antenna gain (dBI)

Manuscript submitted December 13, 1973.

σ = target cross section (dBsm)

R = slant range (nmi)

F = transmitter frequency (MHz)

L_p = propagation losses

L_s = system losses

The 84.15-dB factor includes $(4\pi)^3$ and the required conversion factors. The received power is computed from the radar equation by the NRL version of the ITS propagation computer program.[1,2] This computer program first synthesizes virtual height ionograms from numerical maps of monthly median values of critical frequencies. The ionograms are then used to calculate the elevation of takeoff angle.

(U) The program does not consider ionospheric tilts, so the elevation angle of arrival at the reflector is the same as the takeoff angle from the radar antenna. P_r is computed for transmitter frequencies from 6 MHz to the MUF, every 0.5 MHz apart. The frequency giving the largest P_r, for either the vertically polarized or the horizontally polarized reflector, is considered the predicted optimum frequency for illuminating the reflector. Sections that follow consider the individual components of the radar equation for calculating P_r.

III. TRANSMITTER POWER (U)

(S) The transmitter peak power, P_t, is assumed to be 65.0 dBW. The standard deviation of this value appears to be about 1 dB. The transmitter is designed to output 600 kW with a 3-millisecond flattened cosine squared pulse at a PRF of 40 pps for frequencies from 6 to 40 MHz. The pulse is on a 10% pedestal with 250 microsecond cosine squared rise and fall times. Thus, the 3-ms pulse of this shape with an average power of 600 kW would have a peak power of 25 ms/2.75 ms x 600 kW = 5.5 MW = 67.4 dBW.

(S) Measurements at the time of acceptance tests were 66.4 dBW, 67.3 dBW, and 67.0 dBW at 6 MHz, 23 MHz and 40 MHz, respectively. The peak transmitted power was measured each day during March as part of the morning operability tests. The power varied from 64.3 to 65.9 dBW, with the average being 64.9 dBW and the standard deviation being .3 dBW. These power measurements were at the single frequency of 14.88 MHz. The 1-dB standard deviation assumed incorporates both deviation at the single frequency during March and the deviation over the three frequencies during the acceptance tests.

IV. ANTENNA GAIN (U)

(U) The antenna gain, G, is taken from the model measurements shown in Figure 1. These gains represent a composite gain averaged across frequency and beam position. These are the same gains used in the NRL version

of the ITS computer program for predicting ionospheric propagation. Figure 2 shows a comparison between the composite vertical pattern and antenna measurements made by RADC[3] for the vertical pattern of Beam 12. Other beam positions show similar comparisons.

(S) A comparison of the elevation patterns for different frequencies indicate that the ground screen of the antenna is more effective at the lower frequencies than at the higher frequencies. It is expected that the actual elevation pattern of the horizontally polarized antenna is in close agreement with the composite model measurement, because of the minor dependence upon the ground screen for horizontal polarization.

(U) The data are corrected for the frequency dependence of the vertically polarized antenna elevation patterns by considering the difference between composite pattern and actual pattern as being part of the system loss. Also considered as part of the system loss is loss due to the signal being off the azimuth boresight.

V. THE SWITCHED REFLECTORS (U)

(S) The switched reflectors were provided by MITRE Corporation for calibrating the radar system.[4] The four reflectors provided are at

Site	Ground Range	Azimuth	Beam	Azimuth Error
Kautokino, Norway	1194 nmi	22.9°	1	- .1°
Gardermoen, Norway	591 nmi	29.7°	2	- .3°
Dyarbakir, Turkey	1819 nmi	102.5°	12	+2.5°
Adana, Turkey	1690 nmi	109.1°	13	+2.1°

(S) Each switched reflector consists of a vertically polarized antenna, a horizontally polarized antenna, and solid state switches for modulating the antenna gains by alternately connecting to a matched load or short-circuiting the antenna terminals. The gain modulation is imposed upon reflected signals, resulting in harmonics that are double sidebanded about the carrier frequency. The switching frequencies and harmonic frequencies at system PRF's are shown in Table 1. Because the modulating function is square-wave, the power spectrum of the reflected signal falls off as $(1/f)^2$. The spectrum is shown in Figure 3.

(S) The radar cross section of the switched reflectors at the fundamental of the frequency at which antenna terminals are switched (matched load to short) are shown in Figures 4 and 5. The cross sections are computed assuming flat terrain of average soil. The associated error in cross section is estimated to be less than 2 dB for the vertically polarized antenna and less than 1.5 dB for the horizontally polarized antenna.

SITE	KAUTOKINO		GARDERMOEN		DYARBAKIR		ADANA	
POLARIZATION	V	H	V	H	V	H	V	H
SWITCHING FREQUENCY	15.25	62.55	6.25	10.25	15.25	62.55	14.25	16.25
PRF = 40.0								
1 ST =	15.25	17.45	6.25	10.25	15.25	17.45	14.25	16.25
3 RD =	5.75	12.35	18.75	9.25	5.75	12.35	2.75	8.75
5 TH =	3.75	7.25	8.75	11.25	3.75	7.25	8.75	1.25
PRF = 53.3								
1 ST =	15.25	9.22	6.25	10.25	15.25	9.22	14.25	16.25
3 RD =	7.58	25.68	18.75	22.58	7.58	25.68	10.58	4.58
5 TH =	22.92	7.25	22.08	2.08	22.92	7.25	17.92	25.42
PRF = 80.0								
1 ST =	15.25	17.45	6.25	10.25	15.25	17.45	14.25	16.25
3 RD =	34.25	27.65	18.75	30.75	34.25	27.65	37.25	31.25
5 TH =	3.75	7.25	31.25	28.75	3.75	7.25	8.75	1.25
PRF = 60.0								
1 ST =	15.25	62.55	6.25	10.25	15.25	62.55	14.25	16.25
3 RD =	45.75	27.65	18.75	30.75	45.75	27.65	42.75	48.75
5 TH =	76.25	7.25	31.25	51.25	76.25	7.25	71.25	78.75

(S) TABLE 1. Switching Frequencies and Harmonics of the Switched Reflectors

VI. SYSTEM LOSSES (U)

(S) System losses include RF hardware losses and straddling losses.[5] The RF hardware losses are frequency dependent as shown in Figure 6. Straddling losses are due to the signal not being in the center of the antenna's azimuth beam, the center of a receiver range gate, or the center of a doppler analysis filter.

(S) The -3 dB azimuth beamwidth is 7^{o}. The reflector targets are off boresight by $-.1^{o}$, $-.3^{o}$, $\pm 2.5^{o}$, $+2.1^{o}$, for the reflectors in Beams 1, 2, 12, and 13, respectively. Assuming no azimuthal tilts of the ionosphere, these azimuth offsets give approximate two-way losses of 0 dB, .1 dB, and 2 dB, respectively. Antenna pattern measurements indicate that the main azimuthal lobe is essentially the same, regardless of beam position or frequency. However, the secondary azimuthal lobes vary quite largely with beam position and frequency.

(S) The A/D converter samples the receiver output every 250 μs. If the target return is not at its peak value at a sample time, the signal suffers a range straddling loss. With the 500 μs, $\cos^2$ pulse used during the data collection, the maximum range straddling loss is -2.7 dB, and the average range straddling loss is 1.1 dB. Figure 7 shows the receiver response to various width pulses.[6] The loss in peak amplitude is compensated for in the processor.

(S) The signal is separated into doppler bands by a Fourier transform of the range-gated receiver output. The power spectrum response of a Fourier transform output point (equivalent to the output of a doppler analysis filter) is a function of the time weighting applied to the time function being transformed. For the $\cos^2$ weighting normally used, the weighting function and the power spectrum response are shown in Figure 8. The maximum straddling loss is 1.4 dB and the average straddling loss is .6 dB.

VII. EXPECTED NOISE (U)

(U) If a measurement is to be made of reflected signal power, then the signal power should be larger than the noise power. Figures 9 and 10 show expected median noise power in a one-Hertz band for the month of March and a solar sunspot number (SSN) of 60.[7] The noise shown is the larger of manmade noise in a rural area, galactic noise, and atmospheric noise from CCIR worldwide noise maps. Above 20 MHz, galactic noise dominates, whereas below 20 MHz, atmospheric noise usually dominates.

(S) For comparison with measured noise values, the values of Figures 9 and 10 must be increased by the noise bandwidth of the processor. The noise bandwidth of the IF filter and video filter of the receiver is 3185 Hz. With processing after the receiver a 128-point Fourier transform with $\cos^2$ time weighting, the noise bandwidth out of the processor is reduced to 45.2 Hz or 16.5 Hz.

VIII. DATA COLLECTION (U)

(S) The experimental data were collected according to the procedures in the test proposal. The biggest obstacle in following the procedures was finding frequencies with relatively low noise levels. This obstacle can be lessened by the implementation of equipment modifications to increase the sensitivity of the noise monitor receiver and the installation of a HF spectrum analyzer. Such equipment was temporarily installed and operated with techniques devised by CAPT John Amann and CAPT Lyle Vandeventer during a reflector test on 19 April. The use of this equipment found frequencies that had ambient noise levels 0 to 5 dB less than the frequencies found by the random frequency select mode of the radar. It is recommended that CAPT Amann and CAPT Vandeventer install their equipment and techniques for permanent use.

(S) A second limitation in the data collection is the restriction of transmitter frequency to above 12 MHz after 1700 local time on weekdays and after 1200 local time on weekend days. Unfortunately, much of the March data were collected on a Saturday. This limitation was severest for illuminating the Gardermoen reflector in Beam 2 at 591-nmi ground range. During the March collection period, ground illumination was beyond the reflector. Daytime observations on 19 April, between 8 and 11 MHz, showed good coverage and reflector signals 10 to 30 dB above the noise.

(S) Ionospheric support for propagation was precluded on several occasions by magnetic storm activity. Nighttime returns on the northerly beams (Beams 1 and 2) were precluded during every observation by spread frequency auroral returns. Such auroral returns were observed as early as 1400 local time.

(S) Returns from the far-range reflectors in Turkey were often negligible due to the low elevation angles necessary for propagation to these long ranges. With these low angles, both the radar antenna gain and the reflector cross section are greatly reduced. Because of the reduced cross section of the reflector at the low angles, often the reflector is not observed, although aircraft returns are strong and numerous.

(U) Data tapes were only recorded when a reflector signal was observed with a good signal-to-noise ratio. If the reflector signal was weak or not observed, the reason for the lack of visibility is noted in the test log.

IX. DATA PROCESSING (U)

(S) The processing necessary to extract a doppler-shifted signal from noise is crosscorrelation between the received signal and a set of doppler-shifted replicas of the transmitted signal. In the case of a simple pulse-modulated CW such as the AN/FPS-95 Radar Set, the crosscorrelation is

realized by range-gating the output of a receiver matched to the pulse and then performing a Fourier transform of each range-gated output. The frequency side lobes, due to the truncation in time of signals, are reduced by time weighting before transforming. The time weighting does impose a slight loss of efficiency in extracting the signal from the noise.

(S) In the "on-line" processor the Fourier transform is realized by the equivalent of a bank of narrow-band doppler filters. Actually, only a single filter is used and its input is repetitively read out of memory as the filter's center frequency is stepped in doppler. In the "off-line" processor the equivalent processing is done by the fast Fourier transform algorithm (FFT). The FFT can be done either by a computer program in the "off-line" Xerox Sigma 5 computer or in a special-purpose hardware attachment to the Sigma 5, the IEC (Interstate Electronics Corporation) Model 280 SAS (Signal Analysis System). The "on-line" and "off-line" processing are equivalent except for their dynamic ranges. The dynamic range of the "on-line" processor is about 70 dB; that of the "off-line" exceeds 110 dB. The necessity of processing both of backscatter and reflector signals during this test requires the use of the higher dynamic-range "off-line" processor. The "off-line" processing is also preferred because of the greater flexibility in generating the necessary display formats for the processed data.

(S) The receiver output tapes were processed "off-line" by the NRL program, RSP (Radar Signal Processor). The first pass of processing is a 128-point Fourier transform with $\cos^4$ time weighting of each 48 range bins. The range bins are spaced every 500 μs (40 nmi) and are created by averaging two adjacent A/D samples spaced by 250 μs. This processing results in a post-processor noise bandwidth of 58.4 Hz or 17.7 dB Hz.

(U) Two display formats are generated from the processor output. The first is an amplitude vs. range plot of the peak backscattered signal and the median noise power in three 10-Hertz doppler bands, 5 to 15 Hz, 15 to 25 Hz, and 25 to 35 Hz. The plot is an average over ten integration times. An example of this format is shown in Figure 11, with CCIR noise level also indicated. This format is used to determine backscatter coverage on the selected frequency in the area of the switched reflector.

(U) The second format is a doppler-range plot, as in Figure 12. This display is used to measure range and doppler of the switched reflectors for use in the third pass of processing. Switched reflector returns are indicated on Figure 12. Each digit on the plot represents the amplitude above a threshold of the filtered sample for that range and doppler cell. In the case of Figure 12, the digits correspond to 3-dB steps above a threshold of -130 dBm. For example, the digit 2 means the amplitude of that cell is $3 \times 2 = 6$ to $6 + 3 = 9$ dB above -120 dBm, or the amplitude is between -111 and -114 dBm.

(S) The second pass of processing is the same as the first pass, except that samples from three out of every four pulse repetition intervals

are dropped by the processor. This means that the processor is at a PRF of 10 pps instead of 40 pps. Therefore, the doppler bands of 5 to 15, 15 to 25, and 25 to 35 Hz are ambiguous with -5 to +5 Hz. This represents no problem though, as this mode of processing is used to examine the backscatter with higher resolution without requiring the larger memory otherwise necessary with a longer integration time. The display format is a doppler-range as shown in Figure 13. The dashed lines show the variation of peak backscatter doppler with range. With such a display, the modes of propagation can be identified. The doppler shift of the backscatter at the range of the switched reflectors indicate what doppler shift to expect from the reflector signals.

(U) The third pass of processing is of three range bins, spaced by 250 μs (20 nmi) and centered on the range bin of peak reflector signal, as found in the doppler-range output of pass one processing. 40-pps data are processed with a 128-point Fourier transform with $\cos^2$ time weighting. This is an integration time of 128/40 = 3.2 sec. However, because the efficiency of $\cos^2$ weighting is 0.6, i.e.,

$$\left(\int_{-\frac{1}{2}}^{\frac{1}{2}} \cos^2 \pi x dx\right)^2 \Big/ \int_{-\frac{1}{2}}^{\frac{1}{2}} (\cos^2 \pi x) dx$$

and the effective integration time is .66 x 3.2 = 2.1 sec. The noise bandwidth is 3815/(.66 x 128) = 45.2 Hz or 16.5 dB Hz. Processing overlap (i.e., time redundancy) is 3.2, meaning that on the average, each input sample is used in 3.2 transforms. The analysis time is integration time/overlap, or 1 sec with this mode of processing. The display format generated is a doppler-time as shown in Figure 14. Figure 15 is a doppler-time output in which the amplitude is intensified by overprinting each digit a number of times equal to itself.

(S) Prior to this pass of processing, five doppler-range windows are set, one for the backscatter and one each for the first harmonics of the return from the vertically and horizontally polarized switched reflectors. The doppler position and extent are set in accordance with the dopplers measured on the outputs of passes 1 and 2; the windows are wide enough in doppler to allow for minor shifts in doppler frequency. The extent is sufficiently wide to allow for changes in the slant range to the reflector (usually three 20-nmi bins). After each transform, the peak signal in each window is found. The amplitude, doppler, and range of each peak signal is outputted to magnetic tape, the "target tape." This tape is the input to the fourth pass of processing.

(S) The fourth pass of processing (performed by the NRL computer program "Job 53D15") inputs the "target tape" and plots amplitude vs. time plots of peak backscatter and reflector signals. Reflector signal is taken to be the smaller of the two amplitudes from the two windows about the two

first harmonics of a reflector signal. If only reflector signal were present, the two amplitudes would be the same. However, the amplitudes differ because of noise interference, and other targets. The smaller amplitude therefore represents a better estimate of the reflector signal amplitude.

(U) Also during pass 4 of processing, signal statistics are computed and cumulative distributions are plotted on a probability scale. A log-normal distribution gives a straight line on the plot. The backscatter signal in general follows a straight line and is therefore very close to log-normal. An example in Figure 16 shows the amplitude distribution of backscatter over a ten-minute period. The reflector returns also appear log-normal for ten-minute data runs with sufficient signal-to-noise ratio. Usually the reflector has fades into the noise, and the cumulative distribution is then composed of two straight line segments, one for reflector signal and one for noise. Figure 17 shows such a case and how each segment can be extended for finding the mean and standard deviation for both the reflector and the noise, assuming a log-normal distribution for each.

X. DATA OBSERVATIONS AND COMPARISONS (U)

A. Beam 1 (U)

(U) Most of the measurements on the reflector in Beam 1 were made on day 069 (10 March). In the early morning hours auroral activity was present and prevented the reflector from being observed. From 1030 to 1900 the reflector signal was periodically observed and recorded on digital tape. After 1900 the aurora returned and precluded further data collection.

(U) The collected data and "off-line" measurements are tabulated in Table 2. All the power measurements are medians over ten minutes, as described previously in Section IX. The cumulative distributions of the clutter, the noise, and the reflector signals show that each of these variables tend to be log-normally distributed. Both the noise and the clutter have standard deviations of between 2 and 3 dB. The switched reflector, as would be any discrete target, is subject to considerable fading and exhibits standard deviations ranging from 6 to 17 dB.

(S) Figure 18 shows the comparison between the predictions and the measurements. The clutter measurements are consistently lower than predictions. This can be partially explained by the radar coverage shown in Figure 19. In no case was the peak clutter at the same slant range as the reflector return. It appears from Figure 17 that the radar operator attempted to center the coverage about the reflector rather than to peak the clutter at reflector range. This is a common practice when the operator monitors radar coverage by looking on an A-scope that displays the in-phase component of the product detector, a waveform that is a product of amplitude and phase. The phase portion of the waveform should be eliminated, by either displaying IF between the product detector or by displaying (the sum of the

START TIME	DAY OF YEAR	TAPE	FREQUENCY AND POLARIZATION	CLUTTER (-dBm)	NOISE (-dBm)	C/N (-dB)	REFLECTOR V (-dBm)	REFLECTOR H (-dBm)
103539	69	1321	14.695H	62±3	115±3	53	115±9	114±8
131410	69	1645	18.720H	68±3	120±2	52	116±7	117±8
132417	69			61±2	121±3	60	117±17	119±14
151404	69	1928						
153751	74	1190	16.550H	60±3	119±2	59	110±10	114±10
170020	69	2096	16.635H	68±2	117±3	49	113±7	116±6
190146	69	2283	(14.500H) (13.975H)	55±4	104±3	49	97±10	99±10

(U) TABLE 2. Beam 1 Measurements

squares of the in-phase and quadrature components of the product detector output.

(U) A large portion of the difference between predicted clutter and measured clutter would be explained by having used σ^o too large in the prediction computations.

(U) Signal measurements are in good agreement with predictions. The largest difference, 7 dB at 1700, appears to be due to illuminating with a frequency somewhat too high.

(U) The noise measurements were consistently higher than expected. As focusing often enhanced the reflector return to more than 20 dB above the noise floor, little care was taken in locating the "cleanest" frequencies. If the procedures discussed in Section VIII had been available then, the noise floor could have been lowered considerably.

(U) Considerable fading is evidenced by the amplitude-time plots of Figures 22 to 27. Very little of the fading appears to be polarization fading due to Faraday rotation. In fact, in two of the records, 1314 and 1901, the reflections from the vertically and horizontally polarized reflectors are highly correlated, with correlation coefficients of .96 and .93, respectively.

(S) Quite often the reflector signal faded below the noise level for periods exceeding one minute, as evidenced by the record for 1314 hr (Fig. 22). At other times the fading was very rapid such as in the record for 1901 hr (Fig. 27). In this record 20-dB fades were occurring about every 10 seconds. This rapid fading was at a frequency very close to the MUF. In fact, 6 minutes into the record the MUF had fallen below the working frequency and the working frequency had to be lowered .5 MHz.

B. Beam 2 Observations (U)

(S) The major portion of the data collected on the reflector in Beam 2 was taken on day 109 (19 April) with one-hop F1 propagation. On most days in March the reflector's range was too short for radar coverage. Attempts to collect data at nighttime were futile because of the nighttime aurora present in northerly latitudes. The data for day 109 are tabulated in Table 3.

(S) A comparison between predictions and measurements is shown in Figure 20. This comparison is only for the vertically polarized reflector. A larger discrepancy exists between measurements and predictions for the horizontally polarized reflector. The takeoff angle predicted is 18^o and gives a slant range of about 640 nmi, which agrees with measured slant ranges. At an elevation angle of 18^o the vertical reflector should have a cross section of 3 to 5 dB less than the horizontal reflector. The comparison

START TIME	DAY OF YEAR	FREQUENCY AND POLARIZATION	CLUTTER (-dBm)	NOISE (-dBm)	C/N (-dB)	REFLECTOR V (-dBm)	REFLECTOR H (-dBm)
080941	109	8.443H	45±3	103±3	58	98±7	99±6
091131	109	9.326H	59±5	117±3	58	99±5	114±11
092131	109		46±3	107±5	59	95	105
092421	109	9.326H	55			96	106
100257	109	9.300H	55±2			103±5	108±4
104421	109	11.080V	53±3			87±4	104±4
113249	109	9.326V	66±3			107±3	115±3
130315	109	9.300H	59±3			107±6	109±7
132733	109	9.853H	62			112	112
145158	109	8.127H	61±3	118±3	53	112±6	116±6

(S) TABLE 3. Beam 2 Measurements

indicates that the horizontal reflector has a cross section of about 10 to 15 dB lower than expected.

C. Beam 12 Observations (U)

(U) The reflector in Beam 12 was observed, but was extremely intermittent. At the long range of the reflector, the takeoff and arrival angles are less than 4^{o} and both the radar antenna and the reflector have greatly reduced gains. Although the reflector return was weak and intermittent, aircraft echoes were often quite strong at the reflector range. No measurements on the Beam 12 reflector are presented in this report.

D. Beam 13 Observations (U)

(S) The data collected for the reflector in Beam 13 are tabulated in Table 4. Comparison between predictions and measurements for the vertical reflector are shown in Figure 21. Measurements for the horizontal reflector are somewhat lower, as would be expected because of the lower cross section of the horizontal reflector at the low elevation angles involved. During the early morning hours the measurements are 10 to 20 dB higher than predicted. This could occur if ionospheric tilts give a higher angle of arrival at the reflector. This is not unreasonable to expect, as the F2 layer would be lower to the east along the path.

(U) Data were collected for most hours of the day, although during the evening hours the reflector was beyond the range of the radar coverage.

E. Fading and Frequency Diversity (U)

(S) The amplitude-time records indicate similar fading for all of the reflectors. Figures 28 to 31 are amplitude records of data collected in semi-automatic mode on three frequencies, five seconds of data for each dwell. These records indicate that a signal-to-noise improvement of 10 to 15 dB could be realized with frequency diversity.

XI. RECOMMENDATIONS AND CONCLUSION (U)

(S) Because of uncertainties associated with the factors of the radar equation, the value of a switched reflector as a calibrated target is questionable. Some of the uncertainty could be eliminated by transmitting a signal of known power from the reflector antenna and by comparing one-way losses with two-way losses.

(S) The real value of the switched reflectors lie in the fact that they are ever present targets for use in evaluating schemes for improving the target detectability of the system. Frequency diversity, not so much to minimize fading but rather to maximize focusing effects, is an example of one such scheme. Of course, other possibilities include pulse compression, different pulse widths or integration times, frequency management techniques, and new displays.

START TIME	DAY OF YEAR	TAPE	FREQUENCY AND POLARIZATION	CLUTTER (-dBm)	NOISE (-dBm)	C/N (-dB)	REFLECTOR V (-dBm)	REFLECTOR H (-dBm)
0203	80	2538	7.785V	46±3	106±3	60	101±6	106±7
0227	69	785	10.990V	48	119	71	107	115
0309	80	2547	6.873V	47±3	106±3	59	97±9	100±10
0320	80	2551	6.873V	46±3	106±3	60	97±9	102±6
0331	80	2552	6.873V	47±3	106±3	59	93±9	96±10
0534	80	2565	19.917V	64±3	131±3	67	129±9	130±7
0557	80	2569	18.513V	64±3	128±3	64	125±6	126±5
0619	80	2570	18.857V	60±3	124±3	64	117±11	123±6
0640	73	2085	22.140V	62	134	72	126	128
0701	75	1708	16.550V	63	124	61	119	120
0717	80	2572	18.590V	61±3	125±3	64	120±9	123±5
1144	73	1595	25.170V	68	140	72	132	133
1432	69	1926	24.500V	66	140	74	134	134
1630	69	1929	20.740V	60	124	64	119	120

(S) TABLE 4. Beam 13 Measurements

REFERENCES

1. Lucas, D. L. and G. W. Haydon, "MUF-FOT Predictions by Electronic Computers," NBS Report 6789 (May 1961).

2. Headrick, J. M. et al, "Virtual Path Tracing for HF Radar Including an Ionospheric Model," NRL Memo Report 2226 (29 March 1971).

3. Parry, Joseph, "Antenna Patterns Project COBRA MIST," RADC-TS-TM-72-2 (July 1972).

4. Waldman, A., "Configuration of Antennas for Switched Reflectors," MITRE Technical Report Number 2326 (20 March 1972).

5. McGeogh, J. M., "COBRA MIST System Losses," unpublished report (February 1973).

6. Stevens, George, "Averaging for Long-Pulse Operation with Directional Sensitivity Modification," RCA Memo OTM-73 (12 May 1971).

7. Lees, Norman, "Program to Predict Local Expected Noise Values for an HF Radio Receiver at any Location," Project COBRA MIST Computer Program S013.

(Page 16 blank)

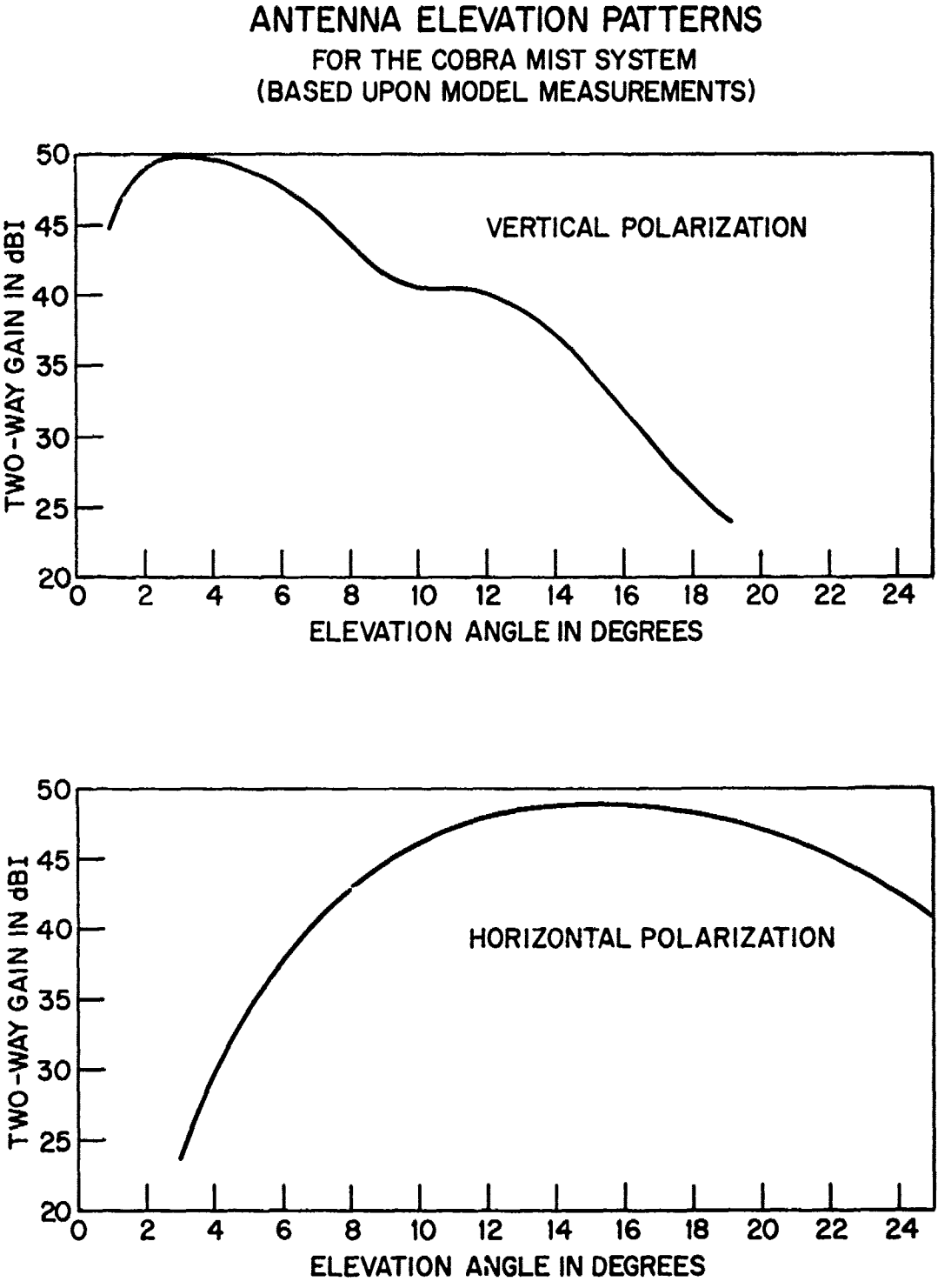

(U) Fig. 1 - Antenna Pattern (Composite from model measurements

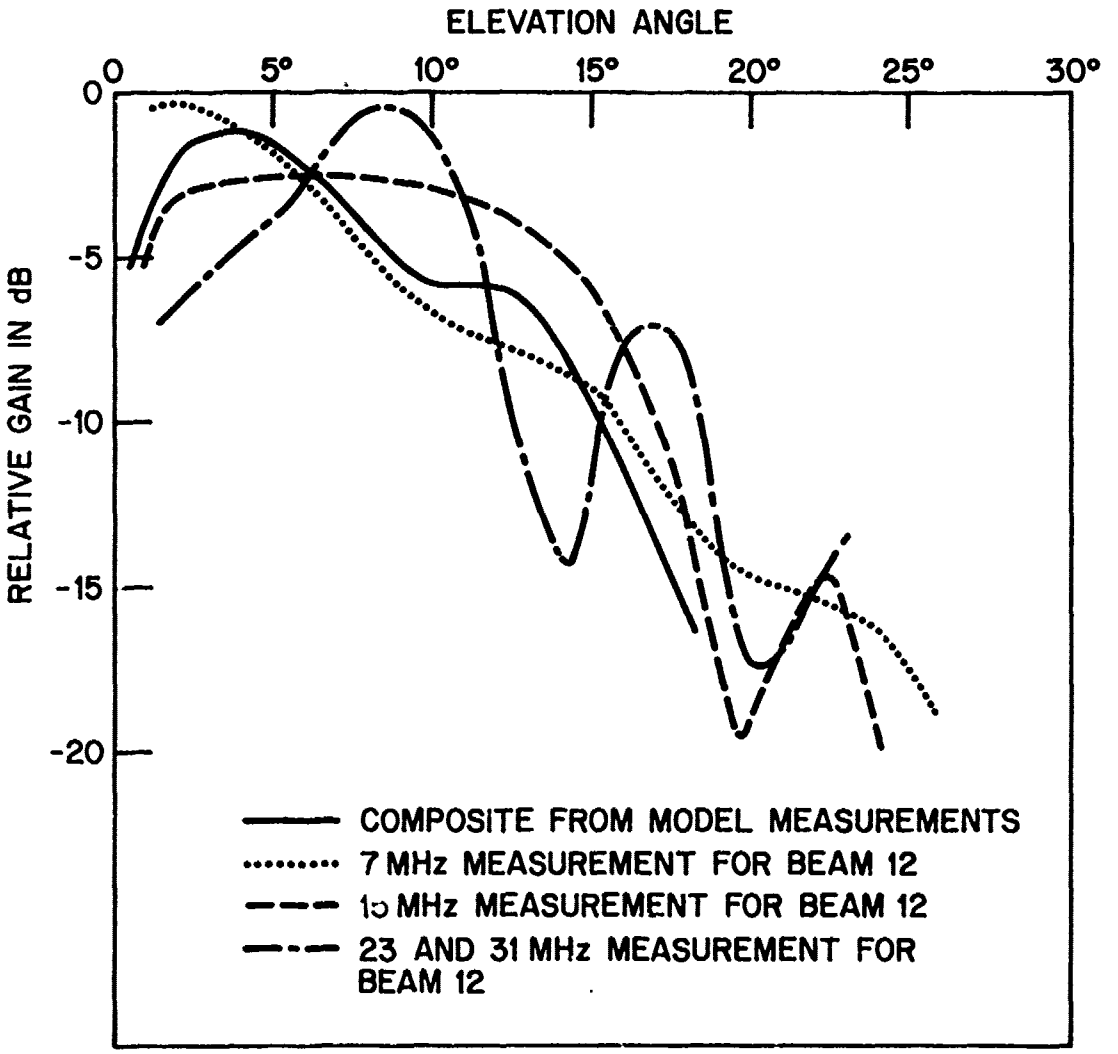

(U) Fig. 2 - Comparison between the composite pattern and RADC measurements

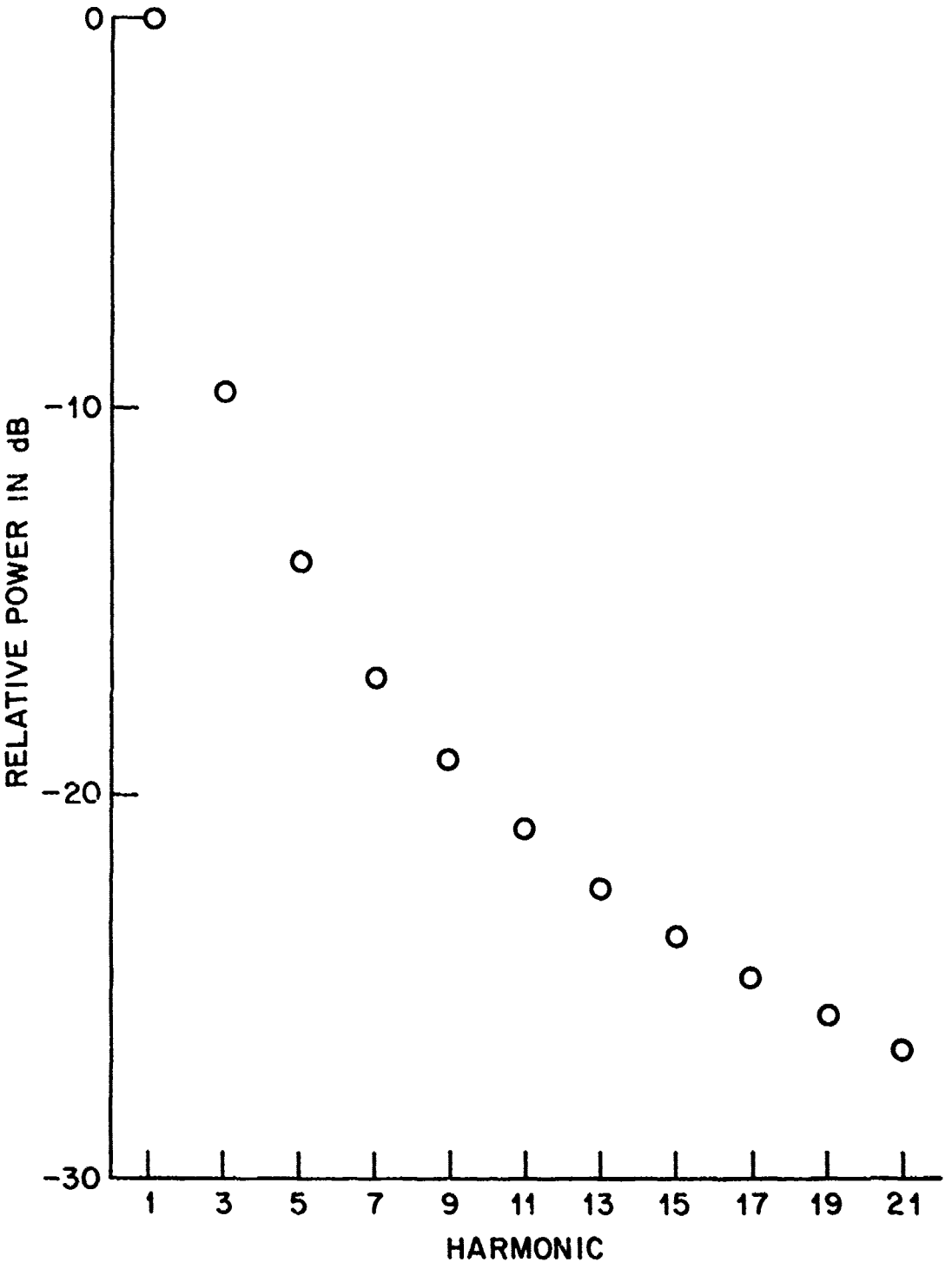

(S) Fig. 3 - Spectrum of reflector signal

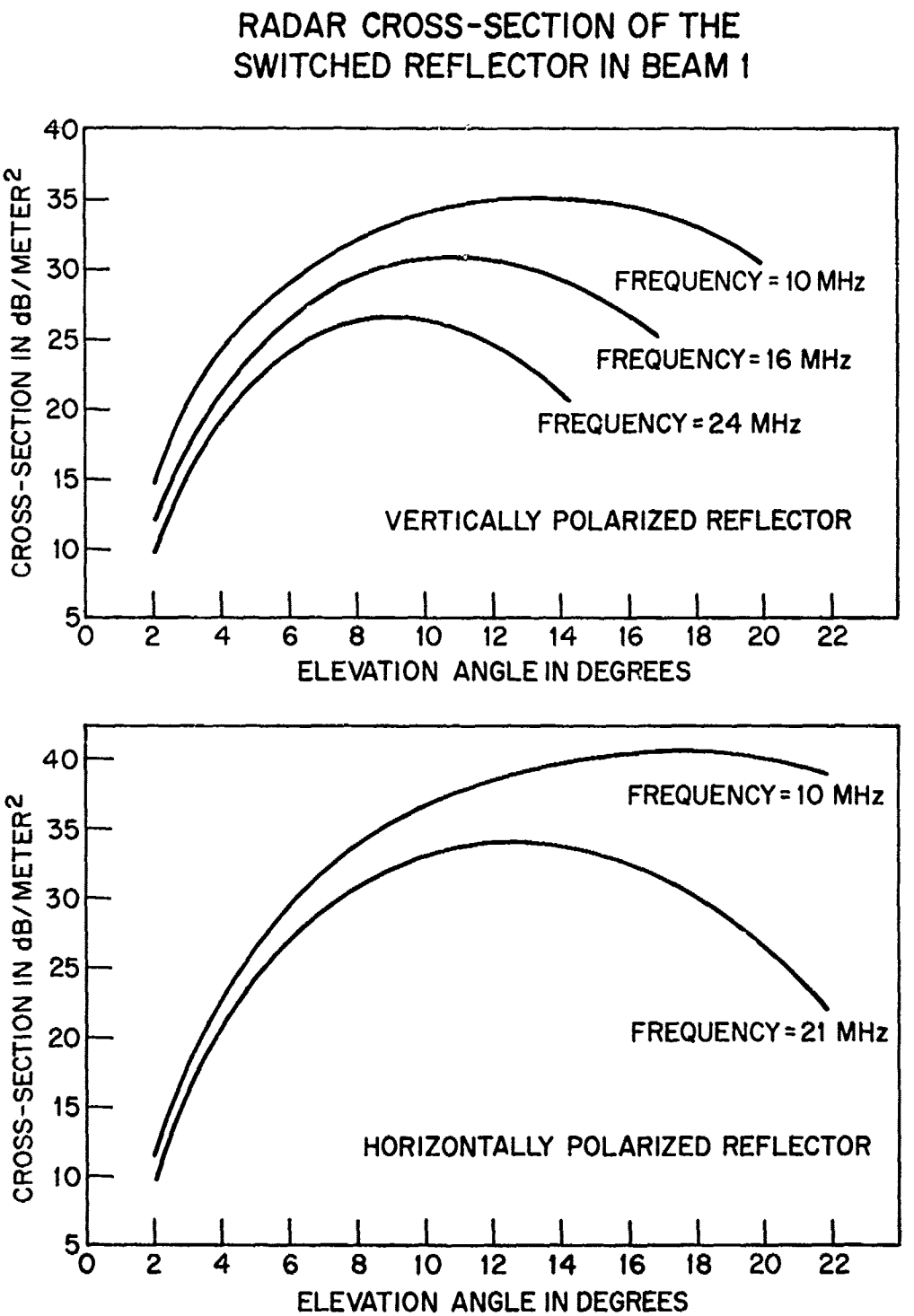

(S) Fig. 4 - Cross-section of reflector in Beams 1 and 13

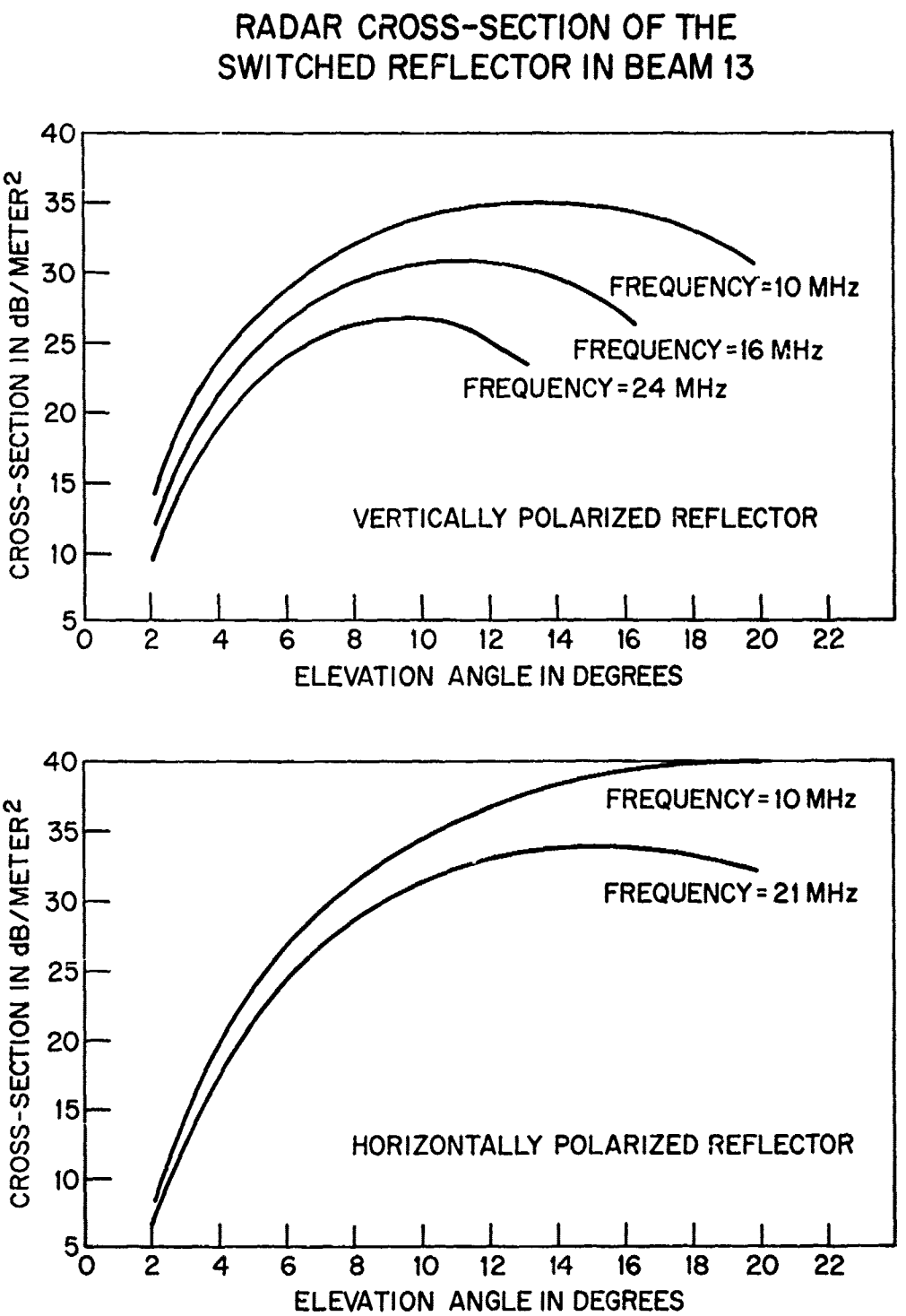

(S) Fig. 5 - Cross-section of reflector in Beam 13

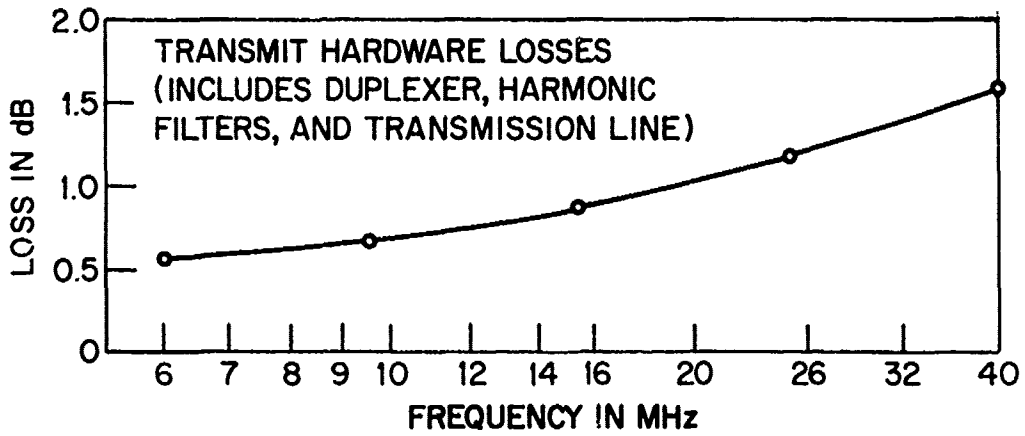

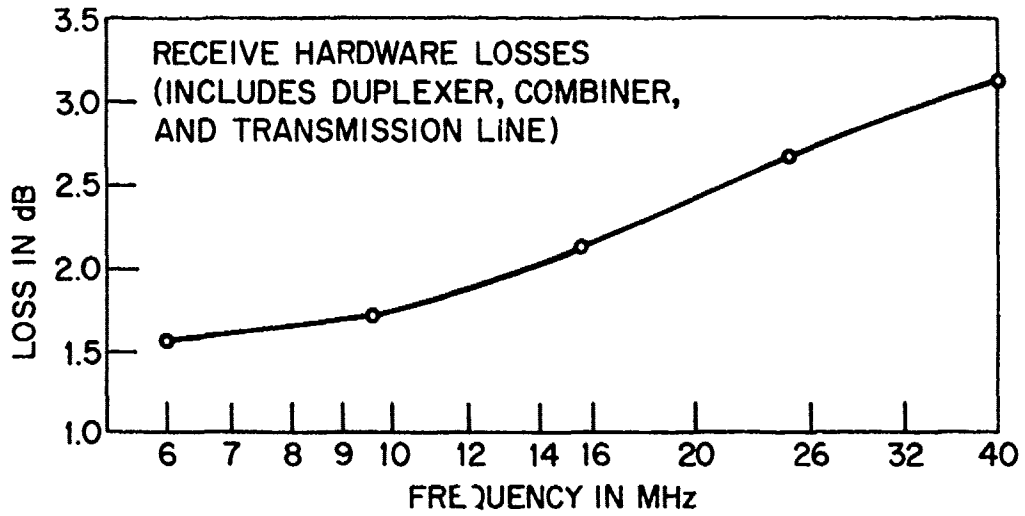

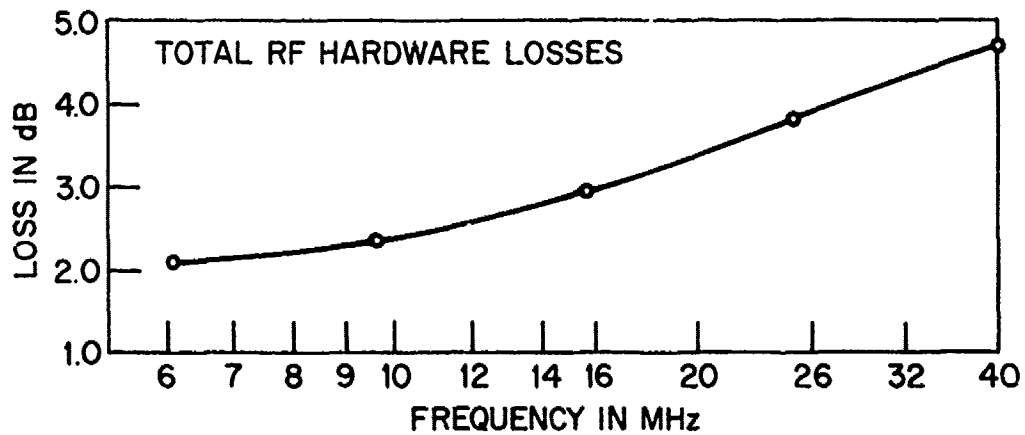

(S) Fig. 6 - RF Hardware losses

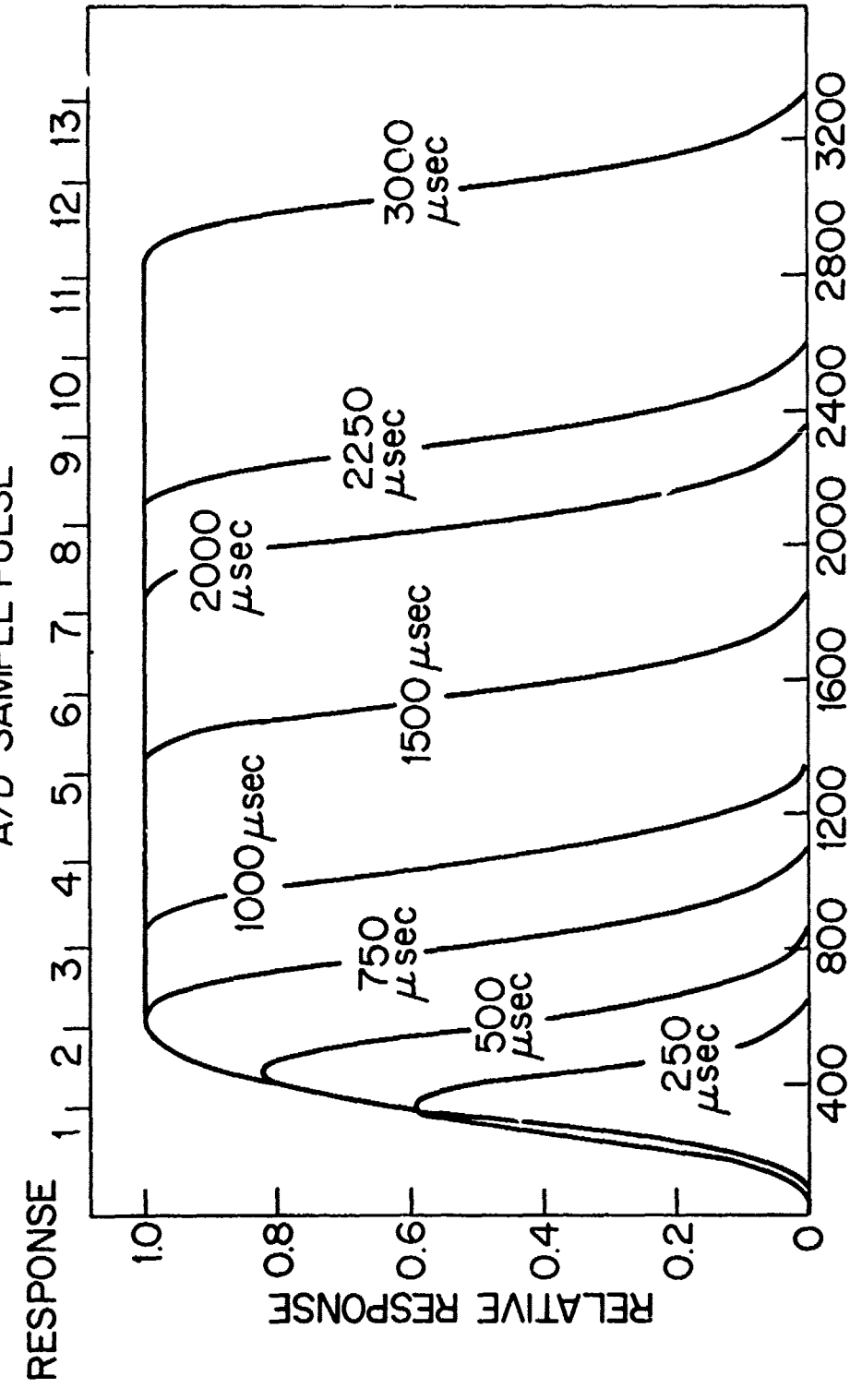

(S) Fig. 7 - Receiver response to pulses

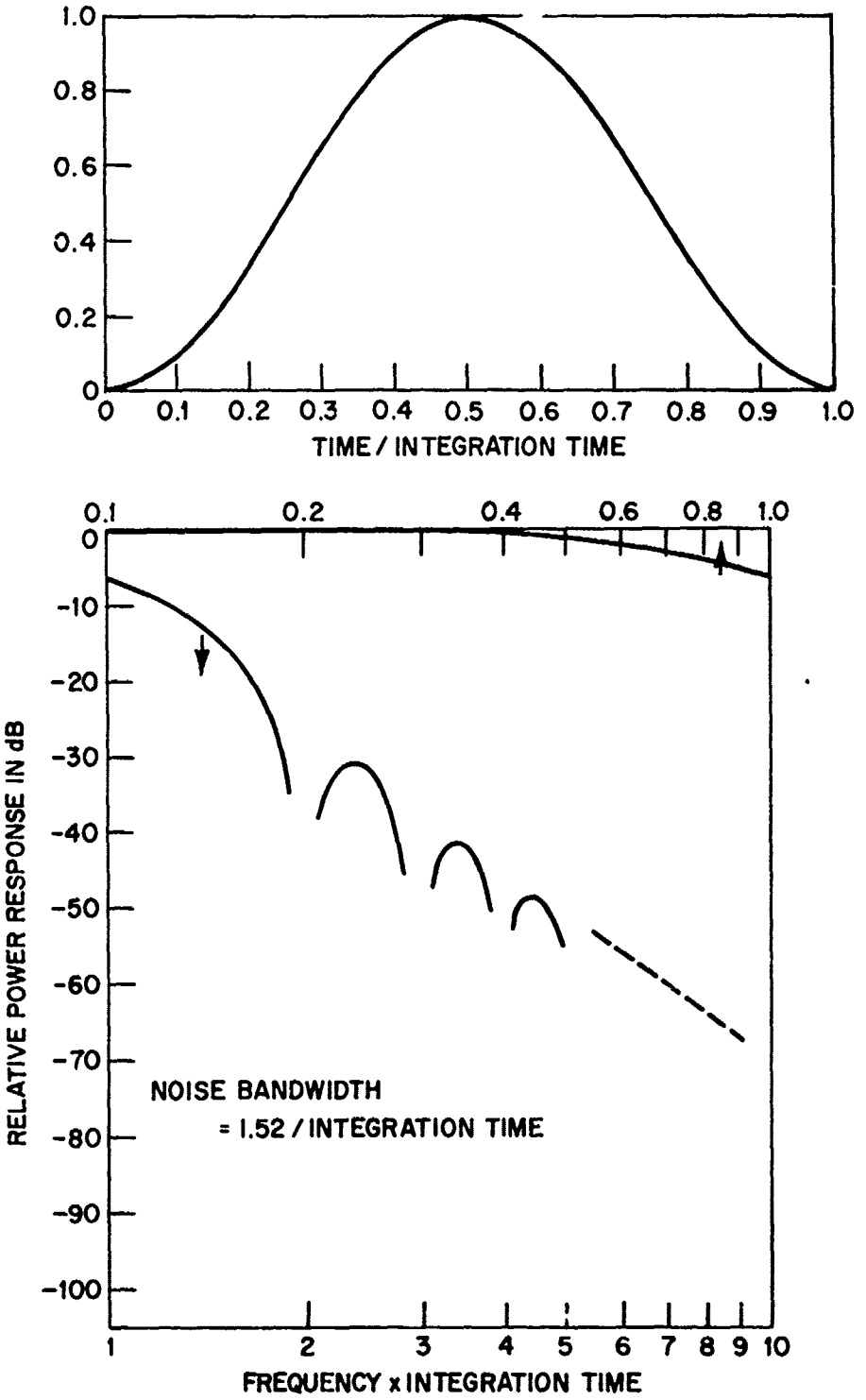

(S) Fig. 8 - Cos^2 time weighting function and response

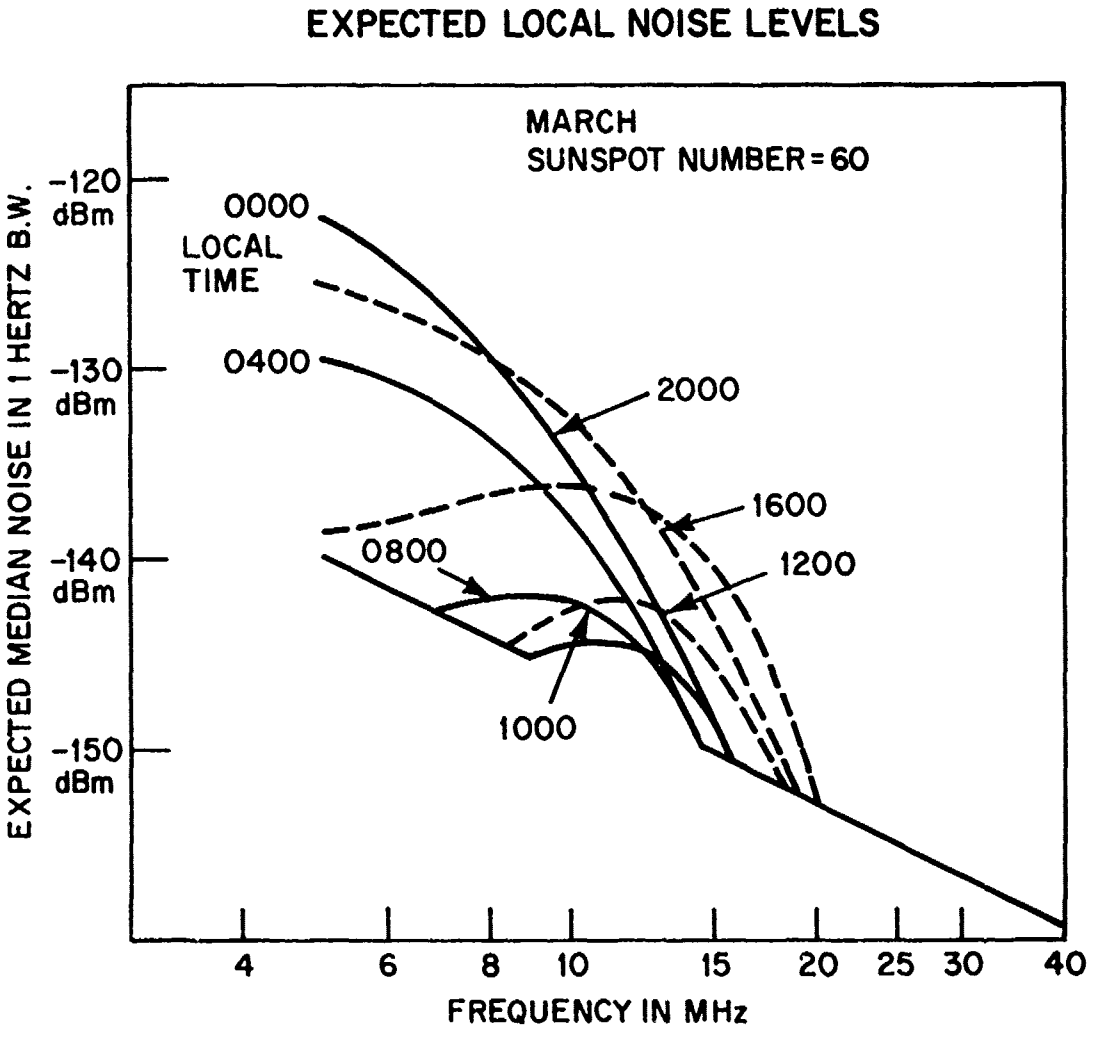

(S) Fig. 9 - Expected median noise power in a 1 Hertz band

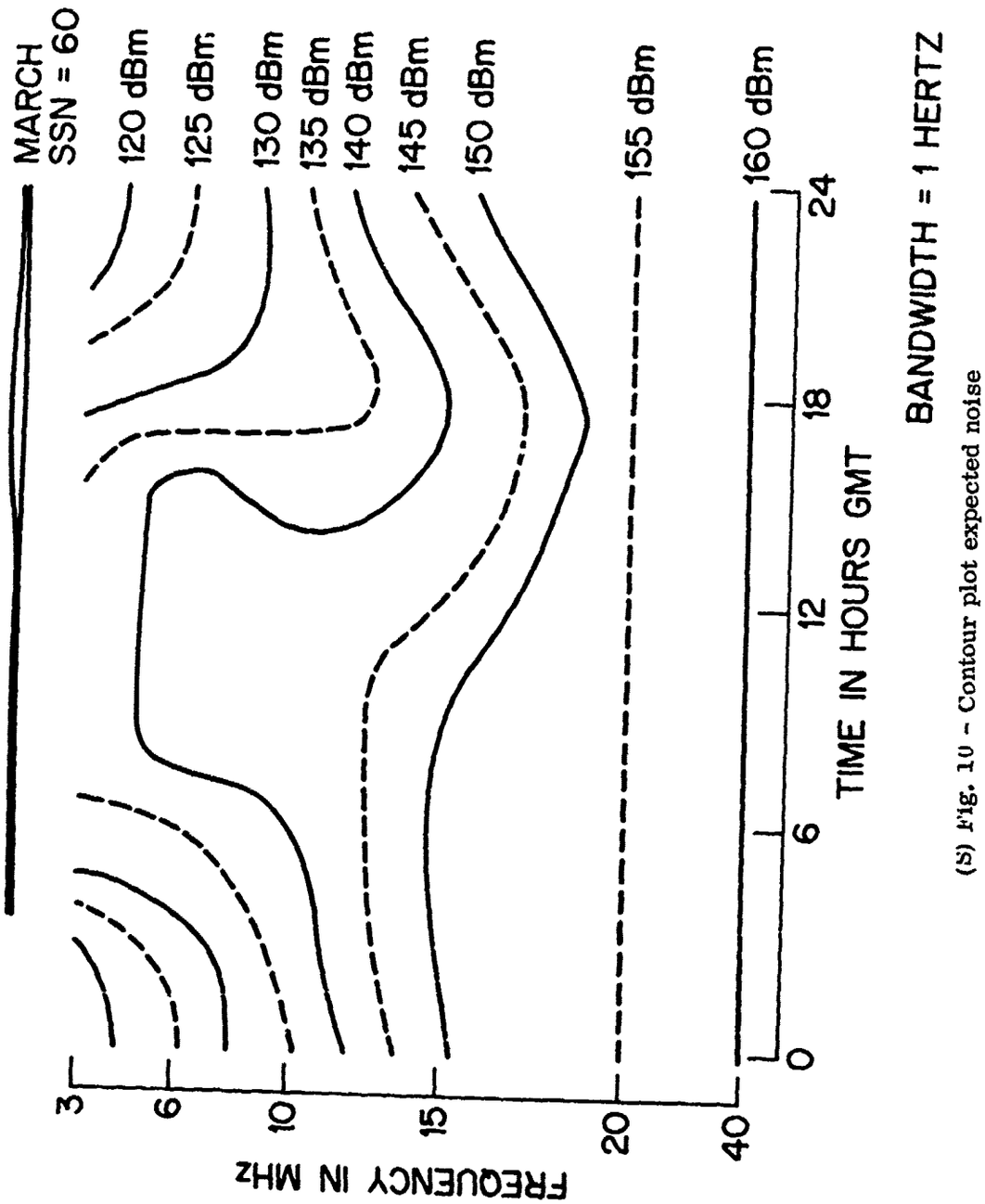

(S) Fig. 10 - Contour plot expected noise

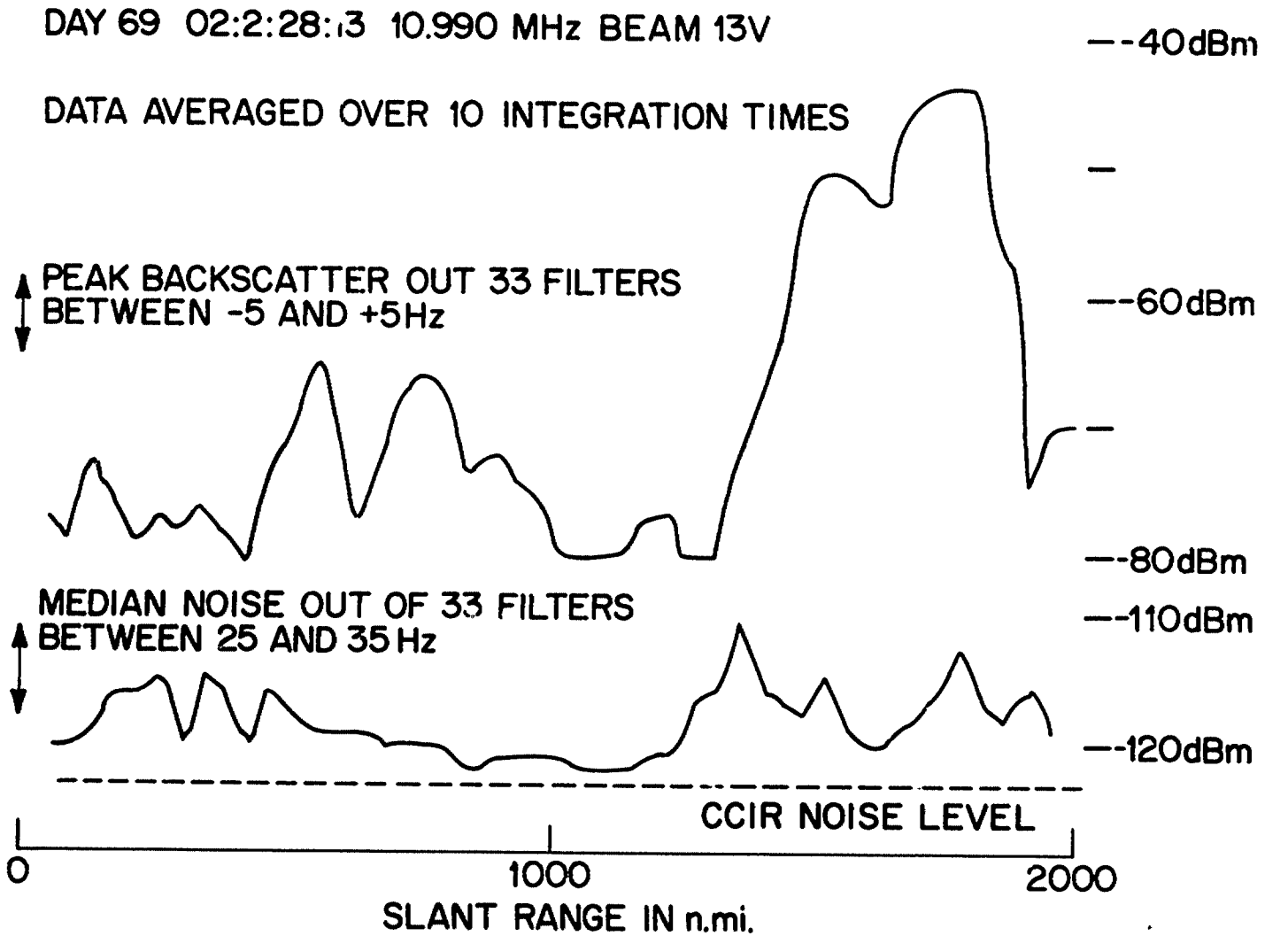

(U) Fig. 11 - Backscatter and noise measurements

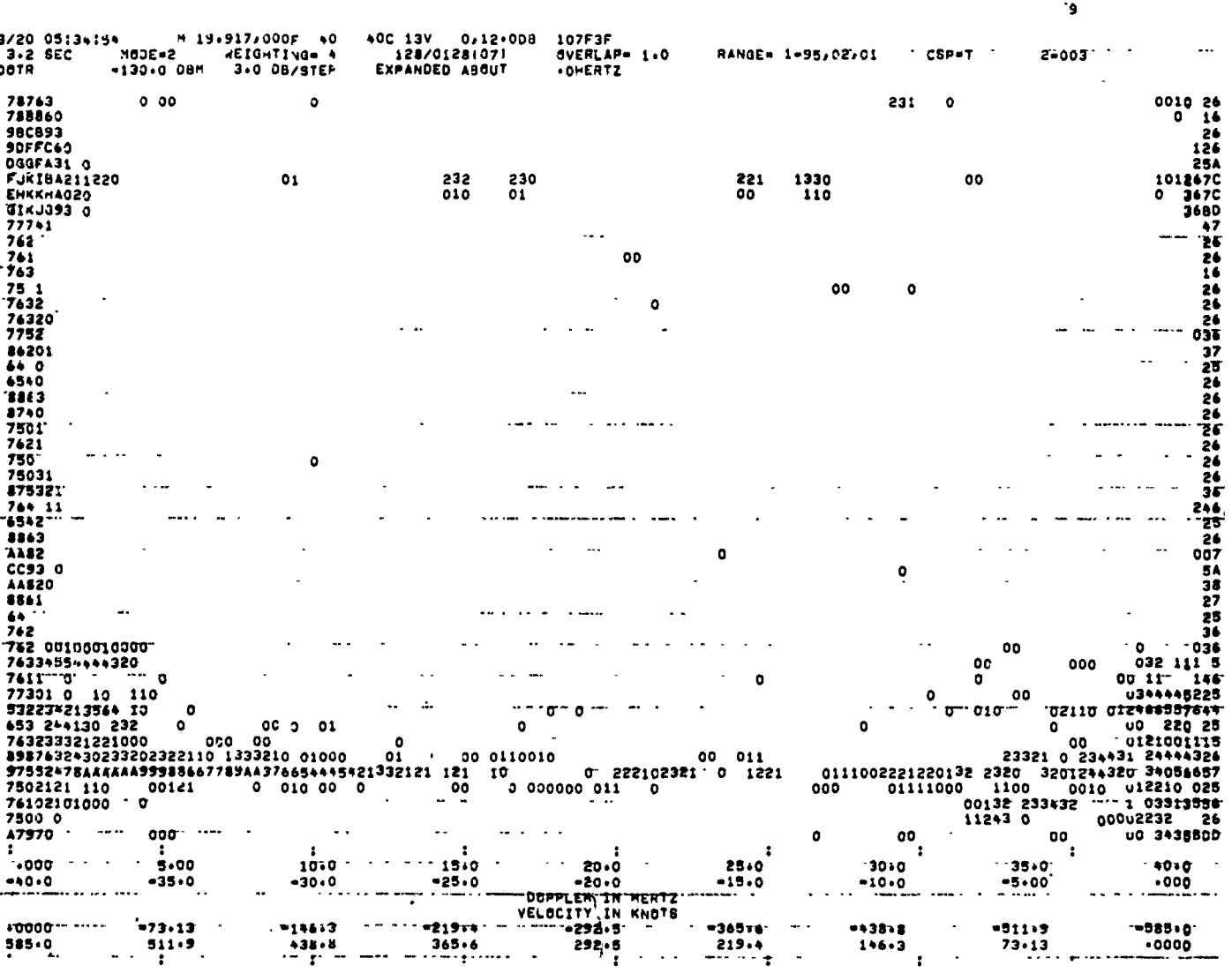

(U) Fig. 12 – Doppler–range radar display

(S) Fig. 13 – Expanded doppler-range

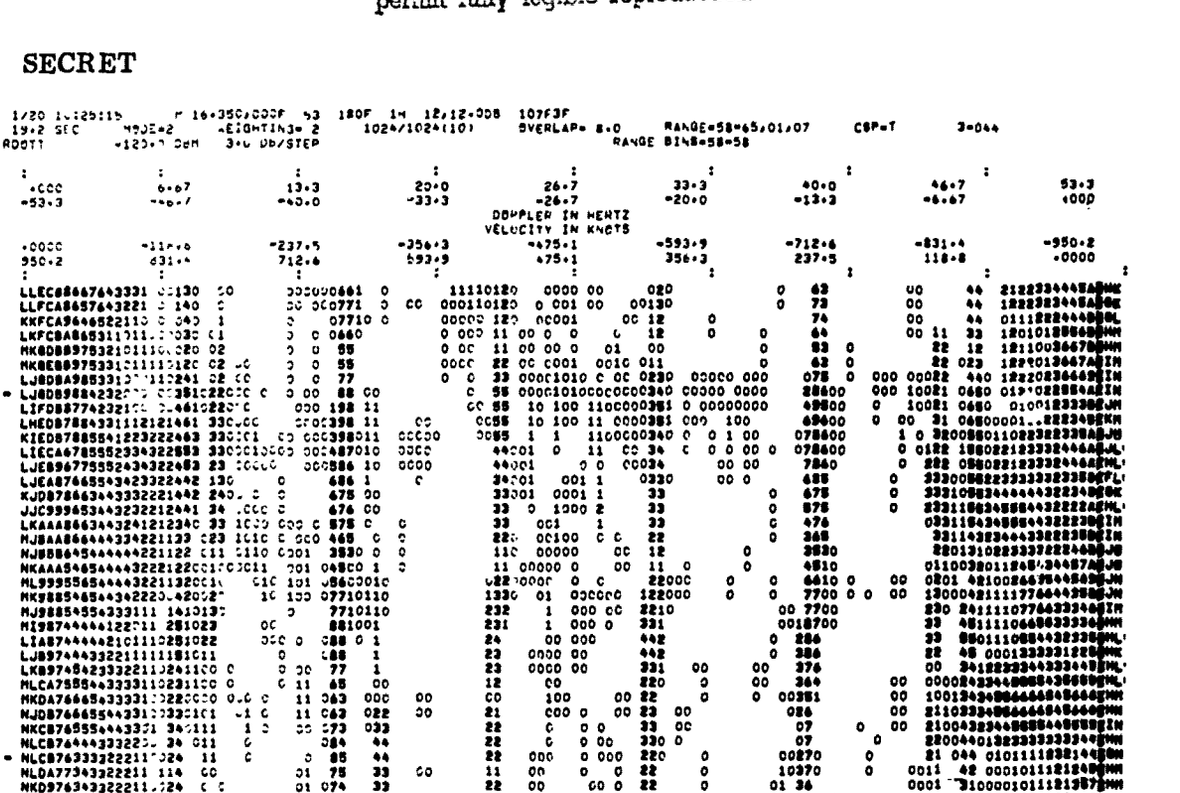

(U) Fig. 14 - Doppler-time display

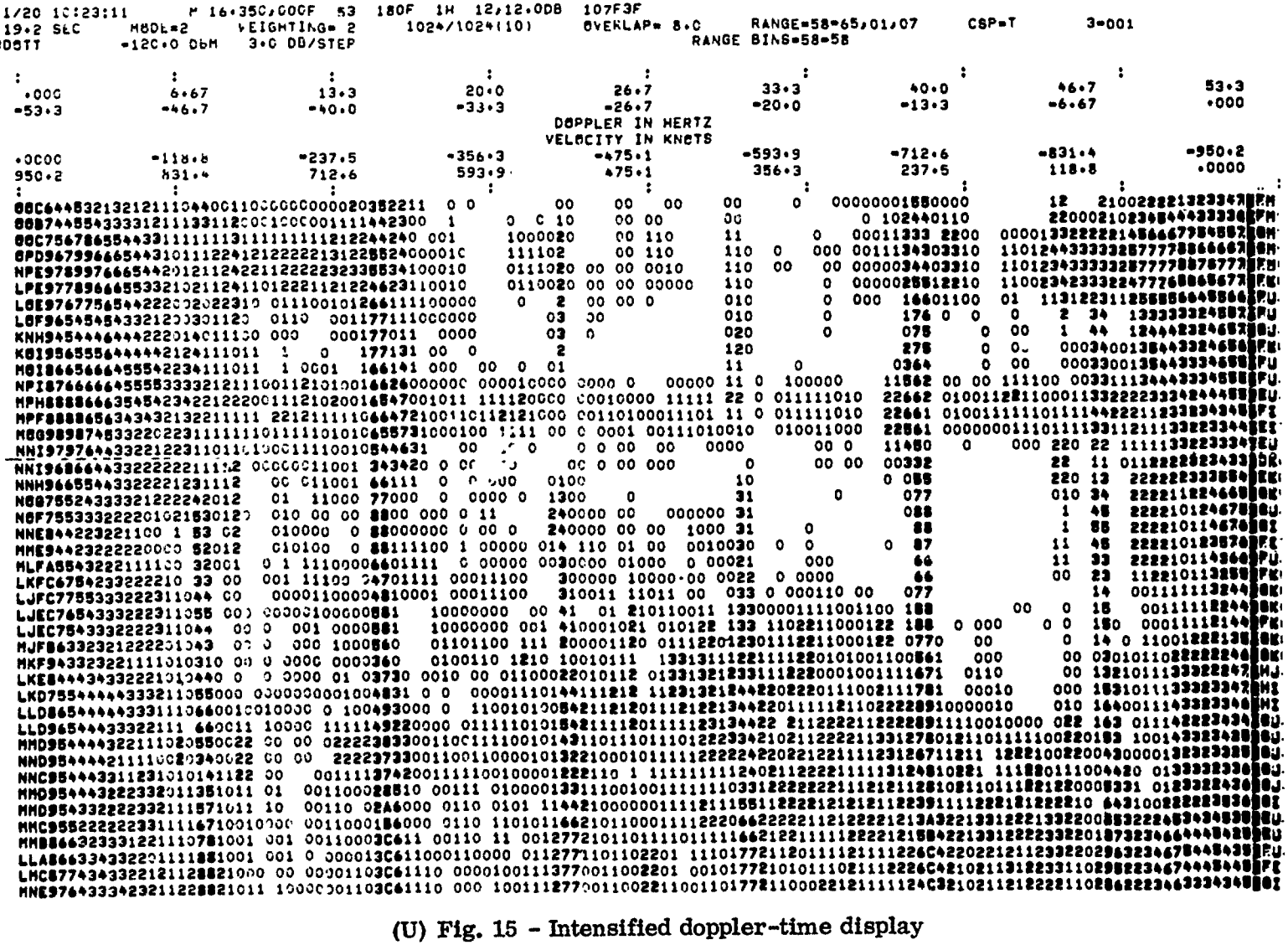

(U) Fig. 15 – Intensified doppler-time display

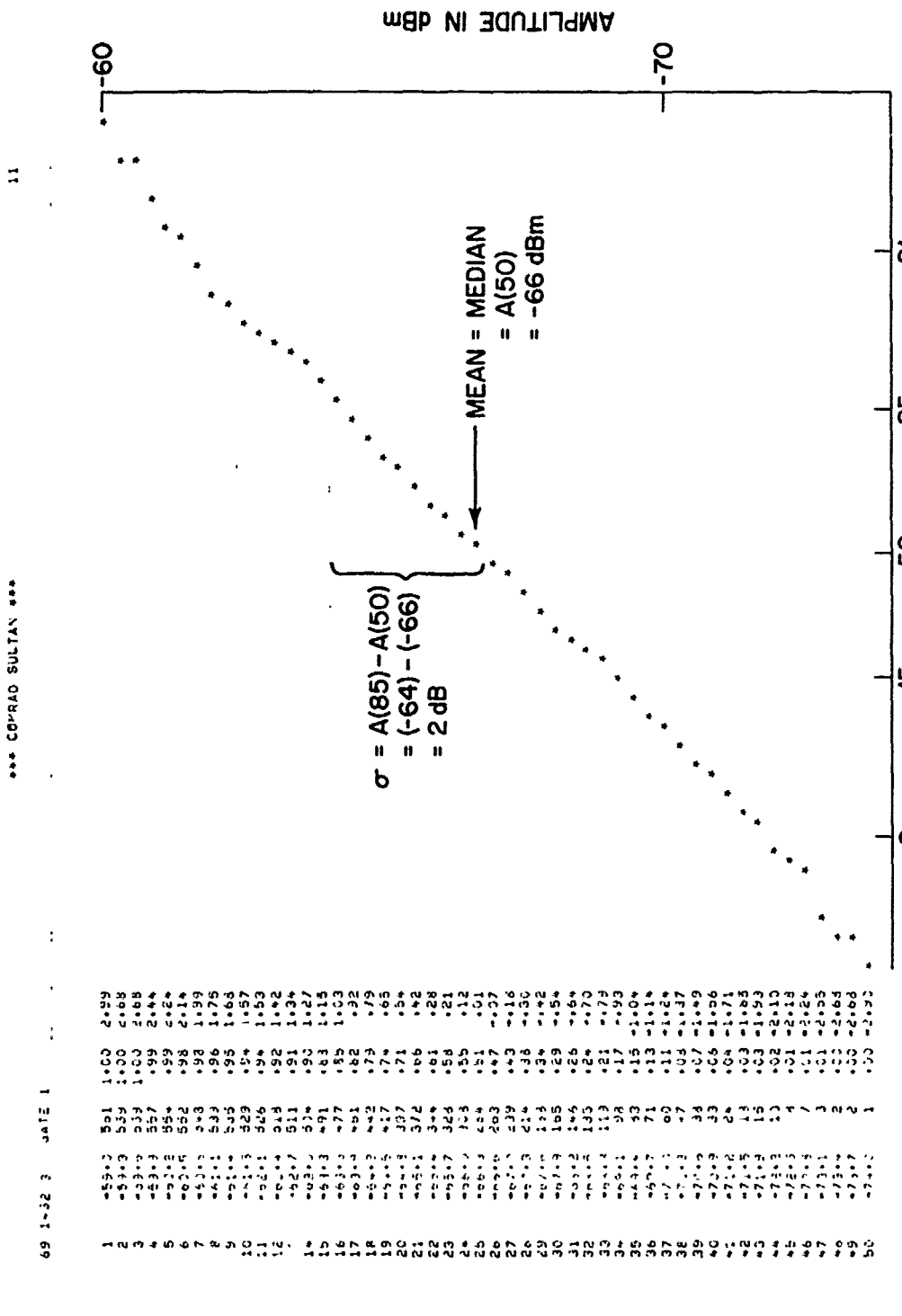

(U) Fig. 16 – Cumulative distribution of backscatter

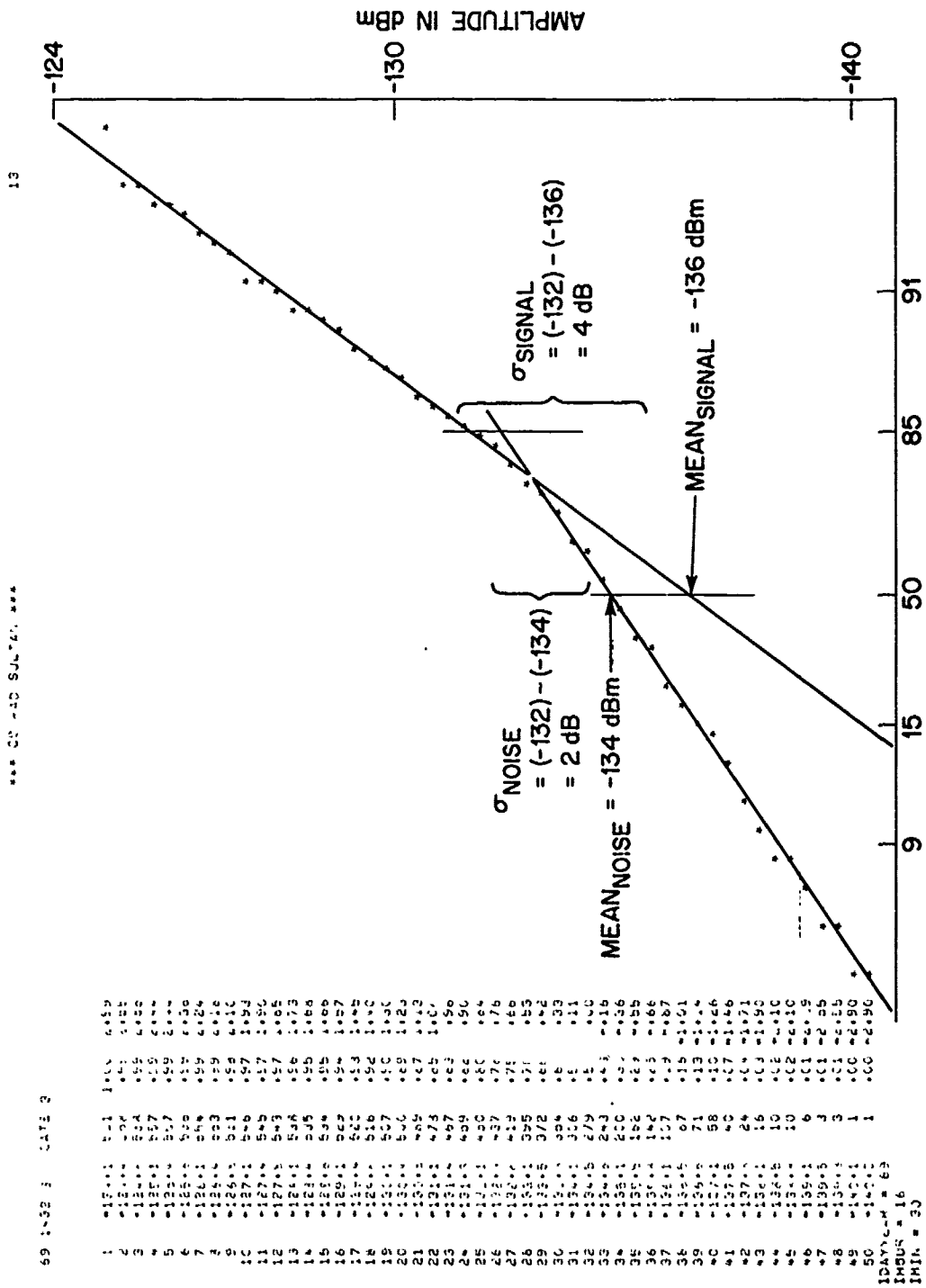

(U) Fig. 17 – Cumulative distribution of a reflector return

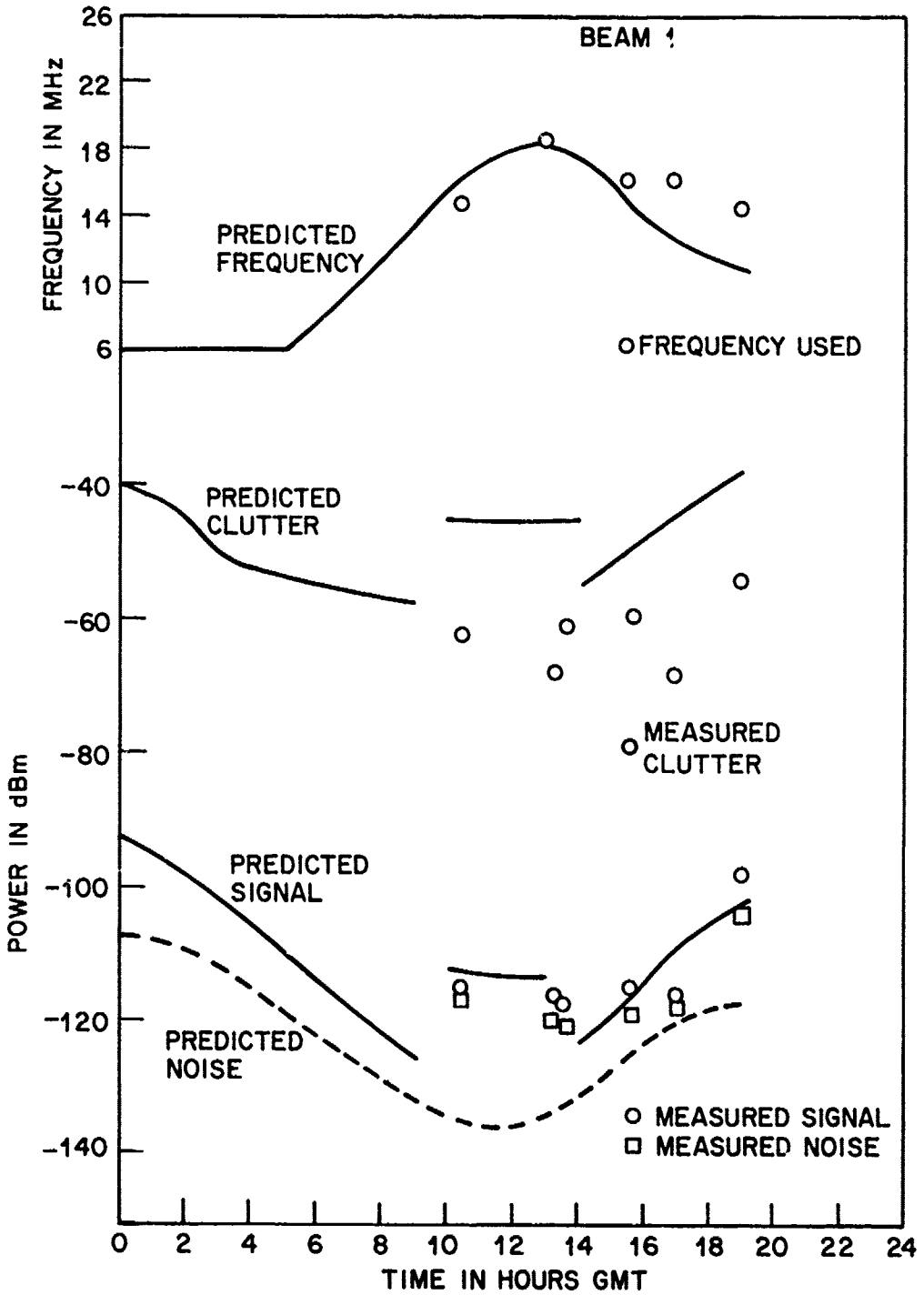

(S) Fig. 18 - Comparison between predictions and measurements

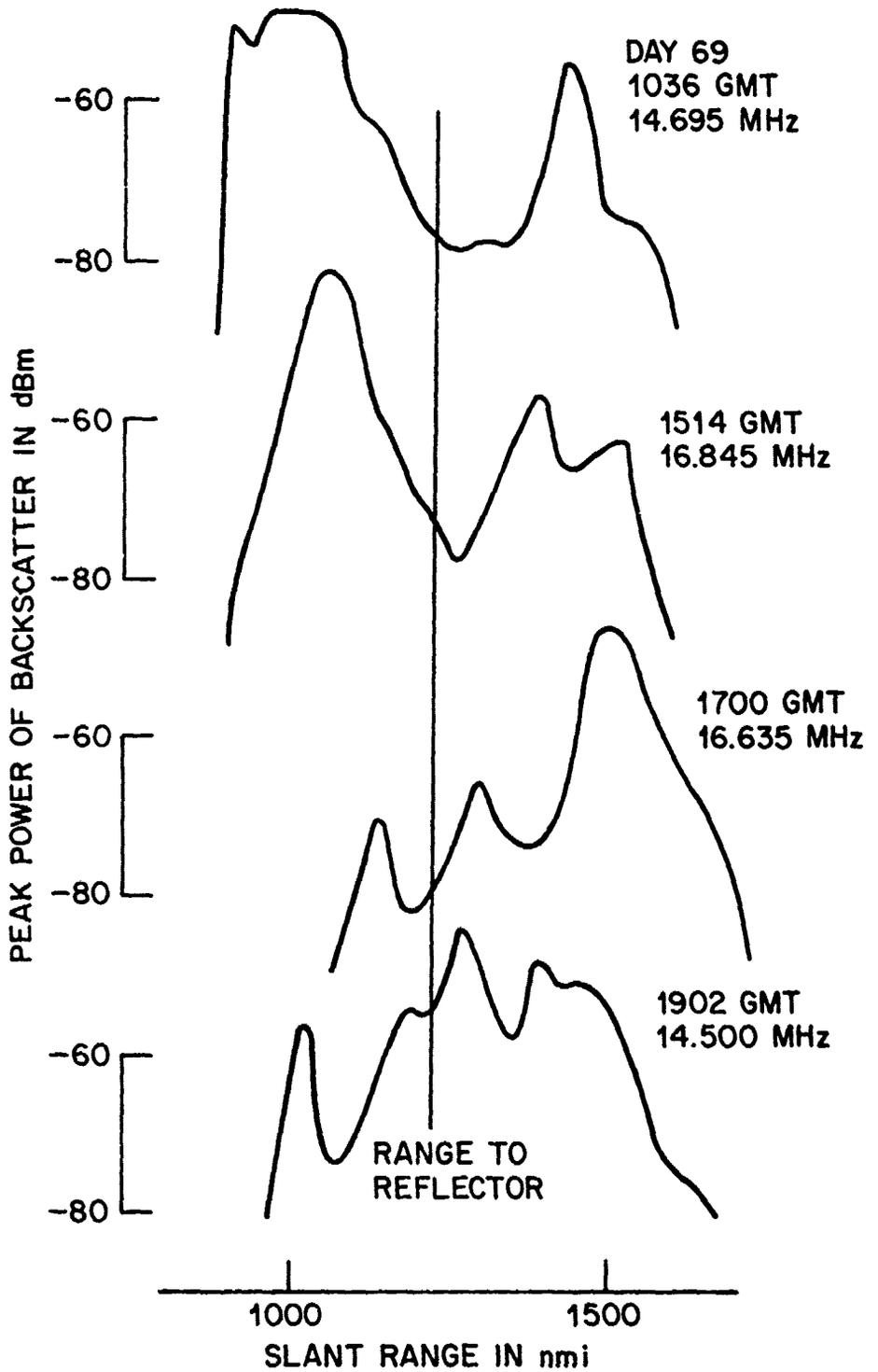

(S) Fig. 19 - Beam backscatter coverage

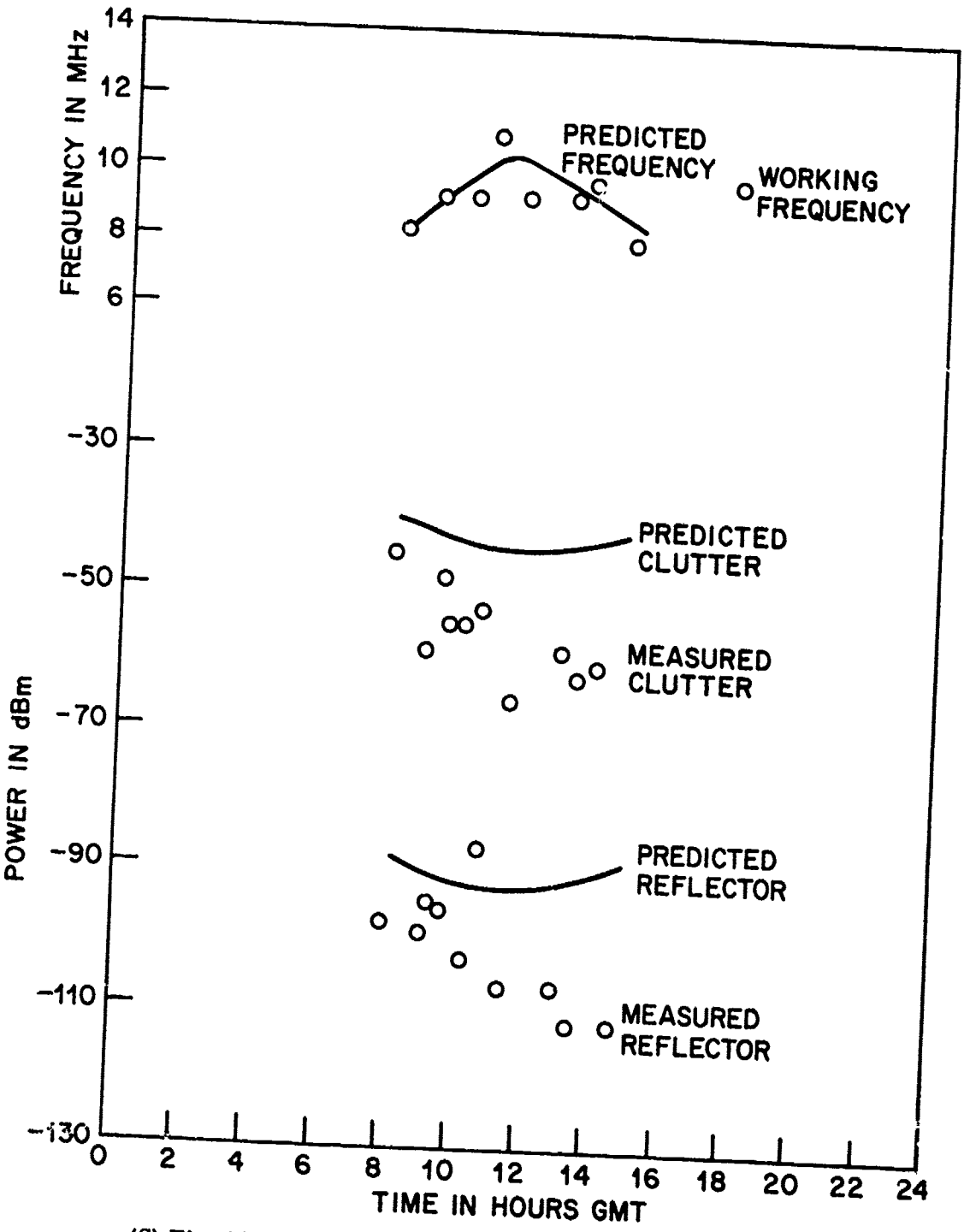

(S) Fig. 20 - Beam 2 comparison between measurements and predictions

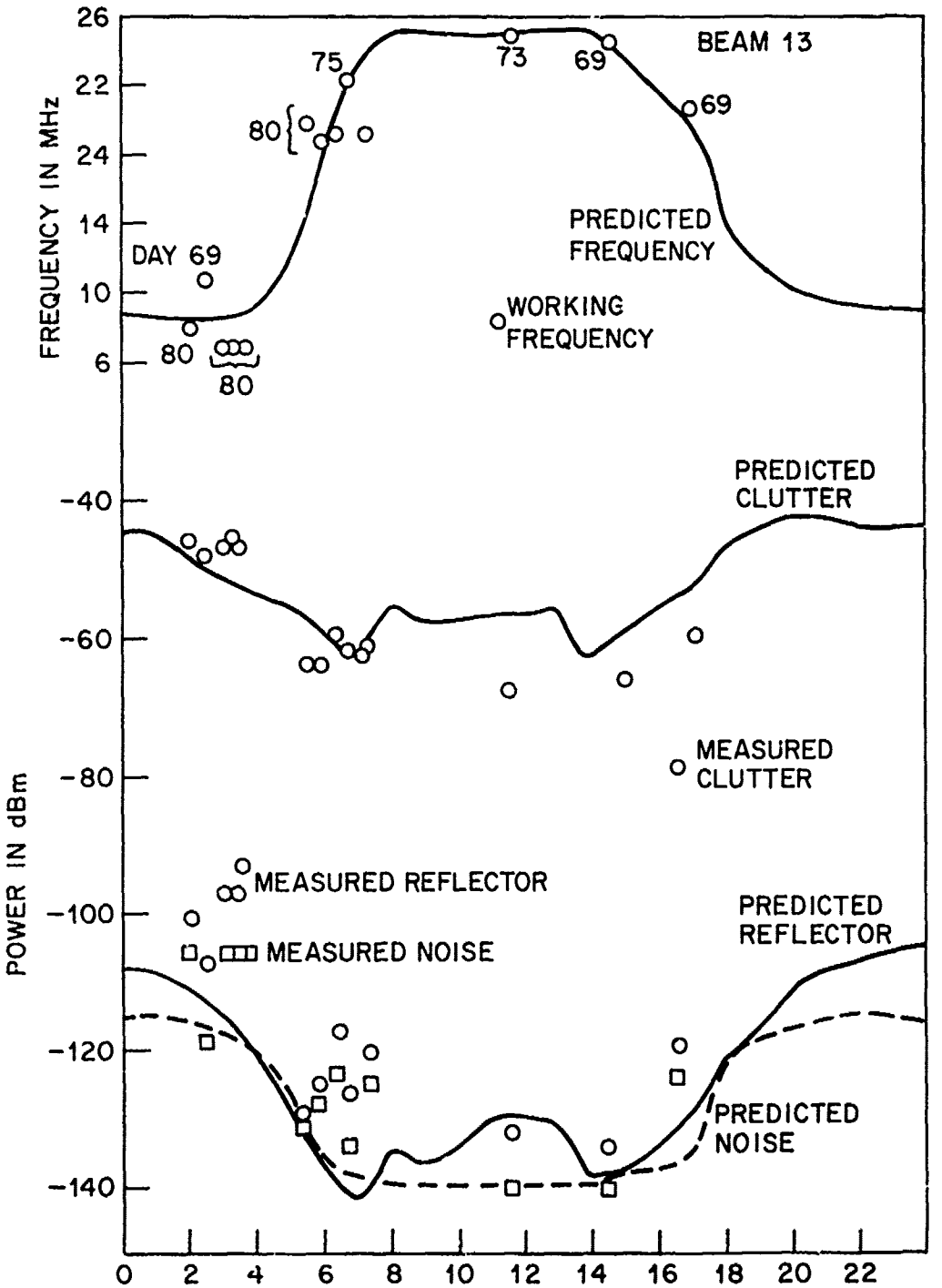

(S) Fig. 21 - Beam 3 comparison between measurements and predictions

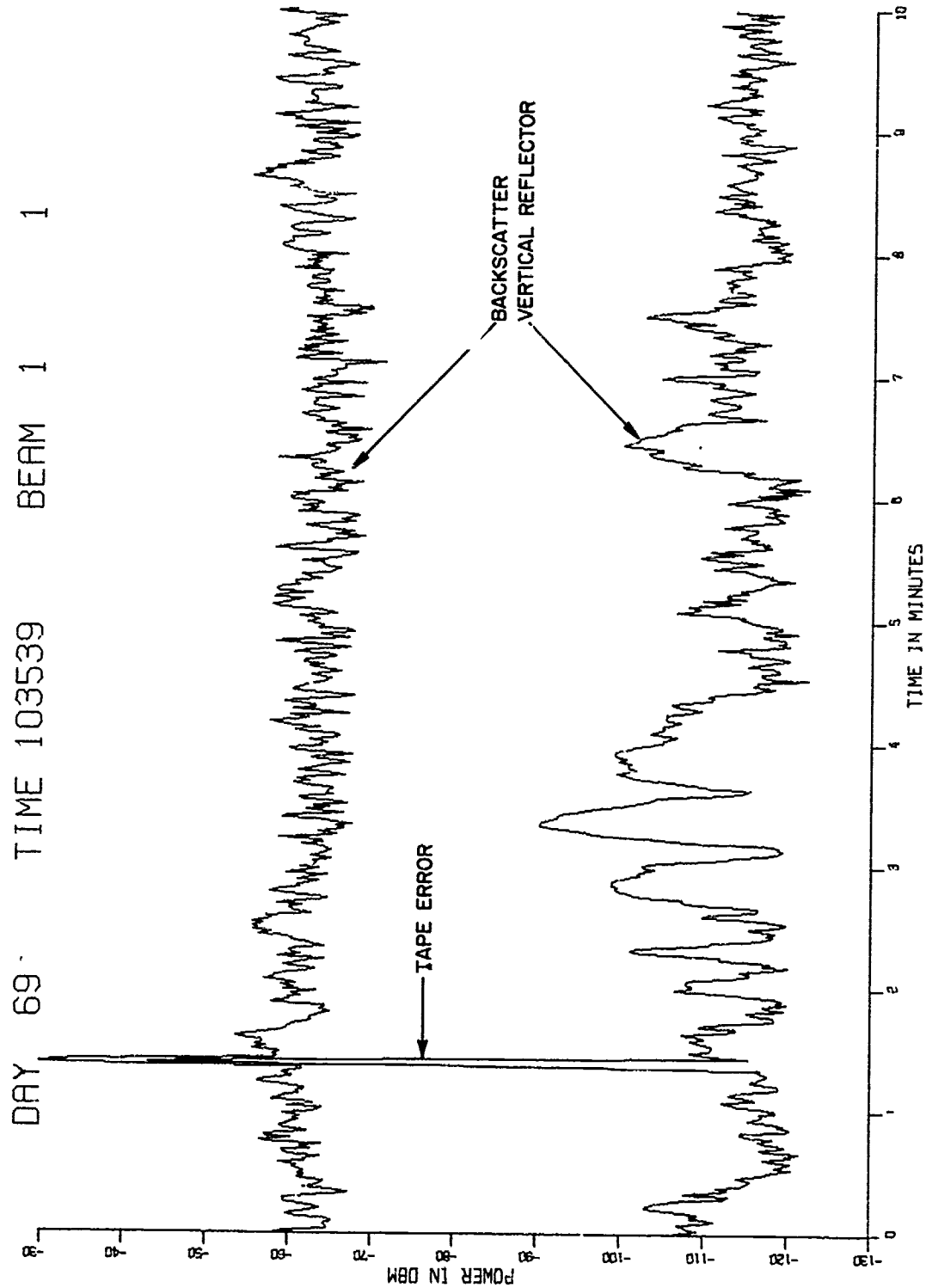

(U) Fig. 22a - Beam 1 at 1035 GMT

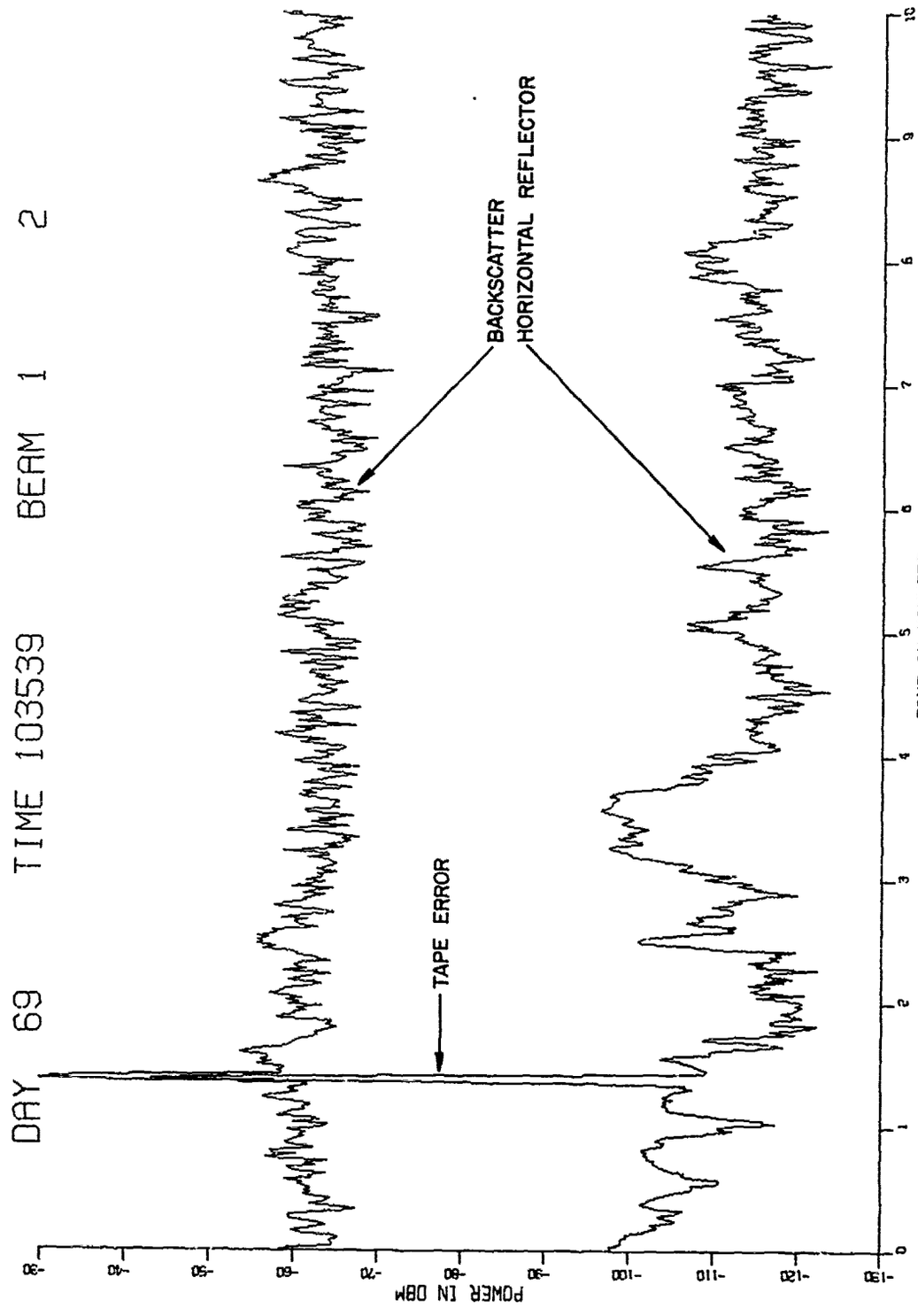

(U) Fig. 22b - Beam 1 at 1035 GMT

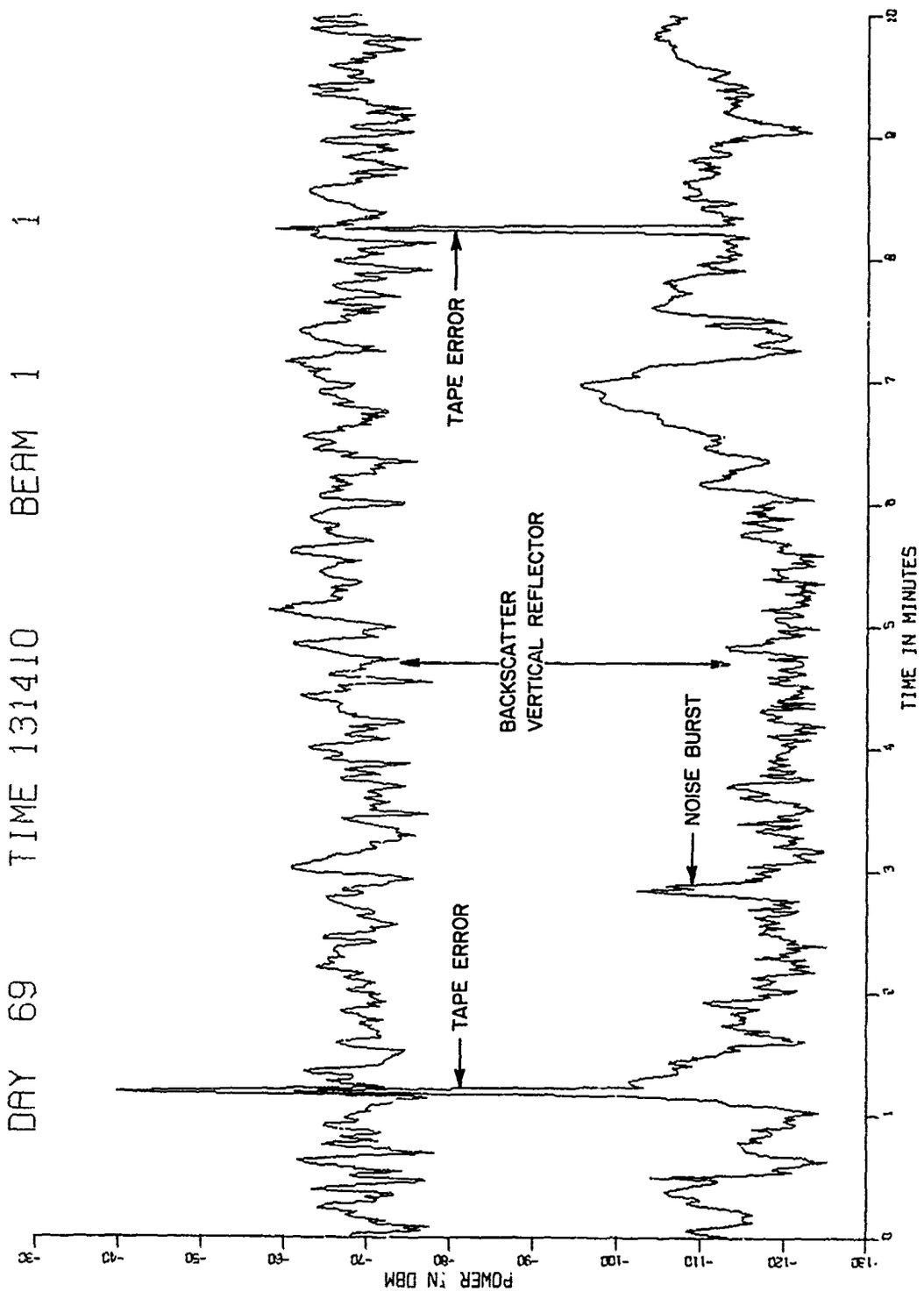

(U) Fig. 23a - Beam 1 at 1314 GMT

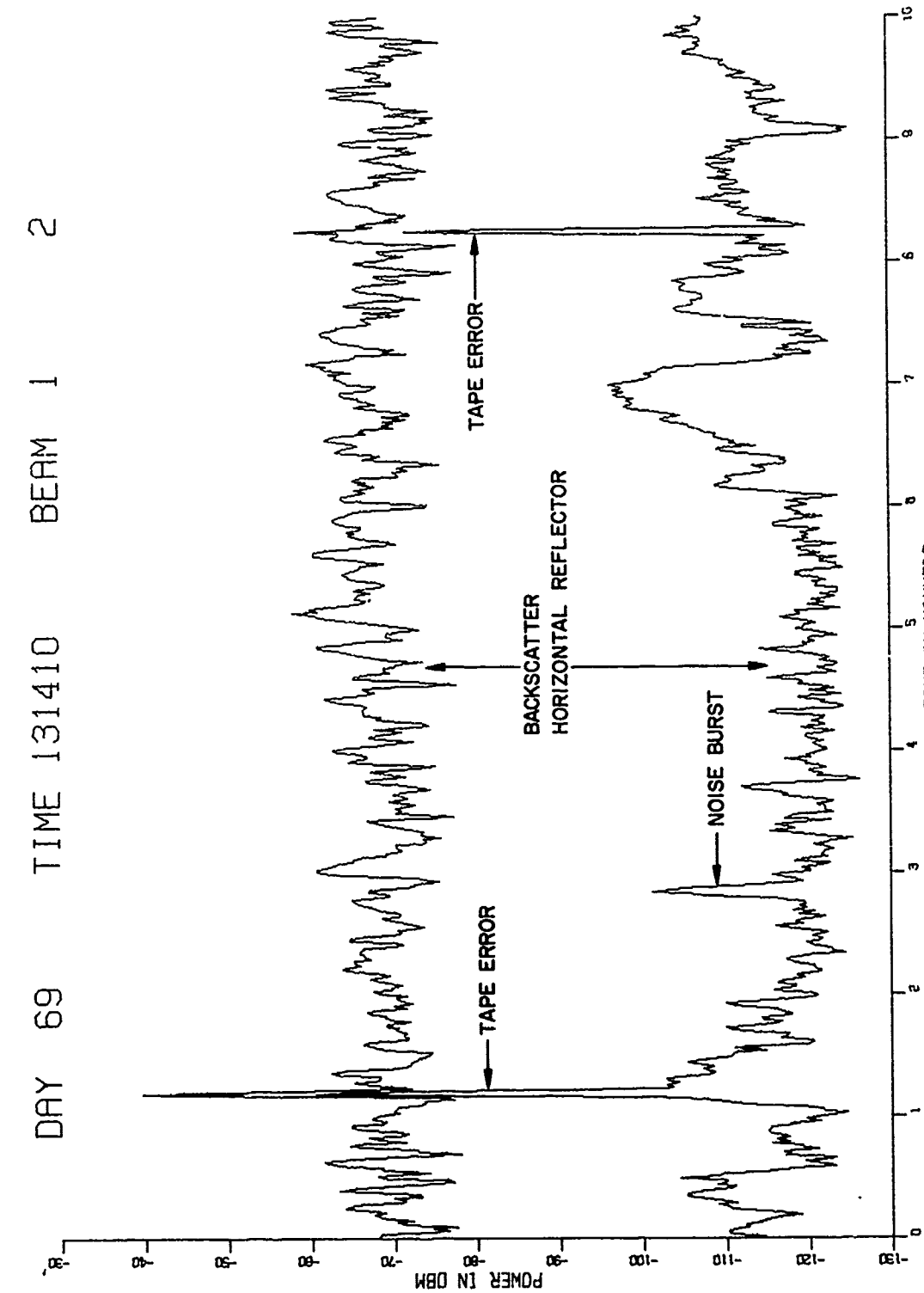

(U) Fig. 23b - Beam 1 at 1314 GMT

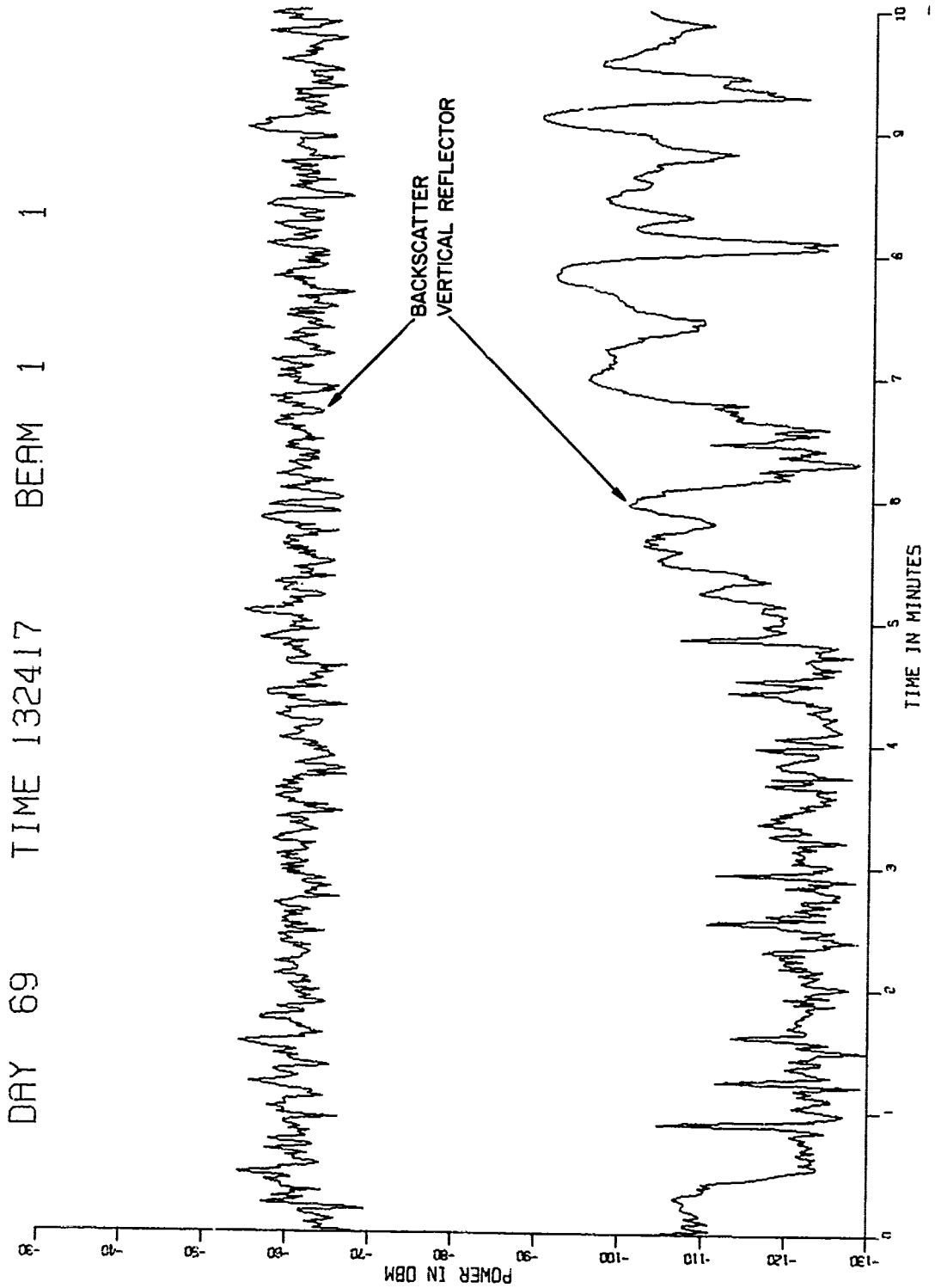

(U) Fig. 24a - Beam 1 at 1324 GMT

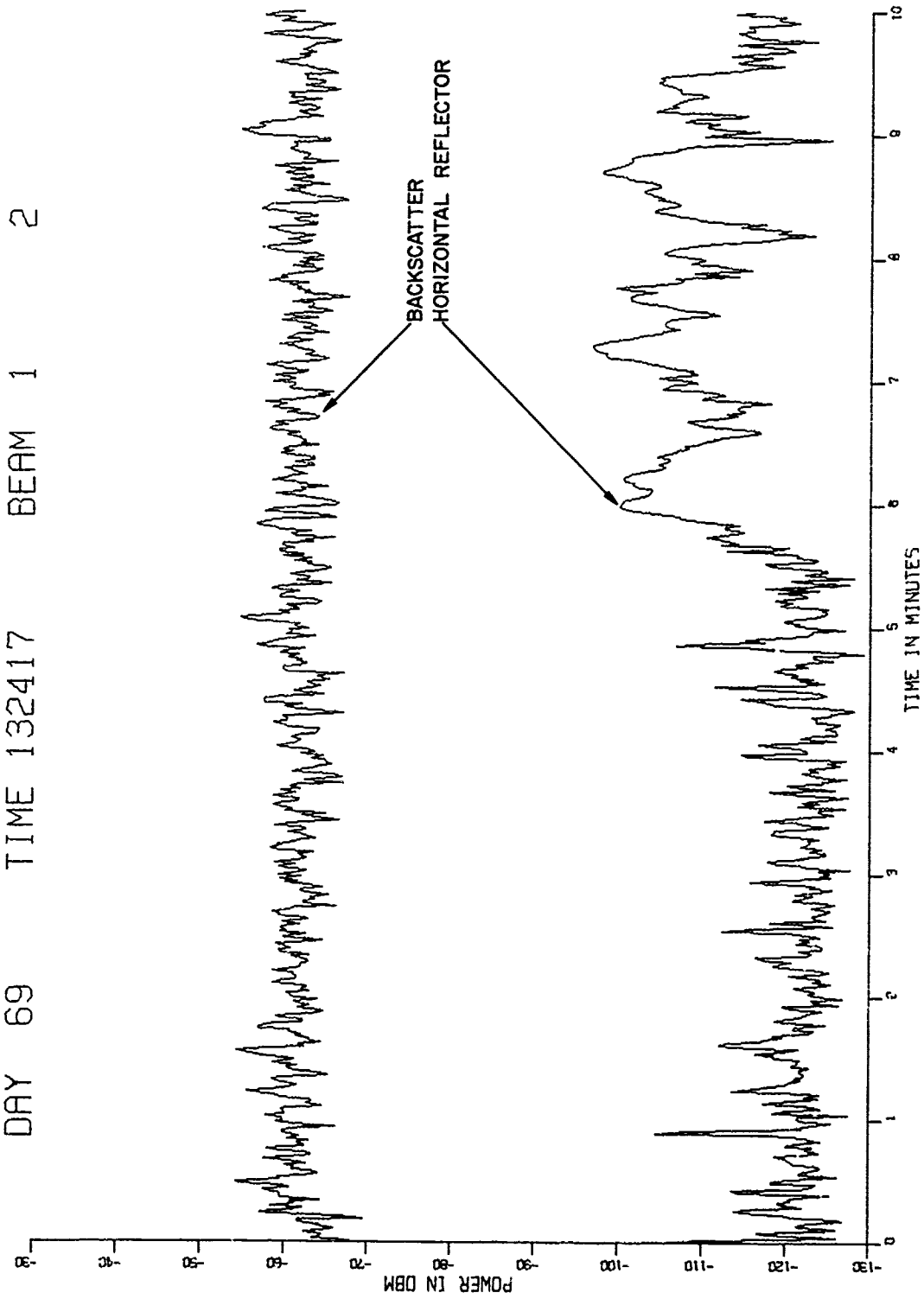

(U) Fig. 24b – Beam 1 at 1324 GMT

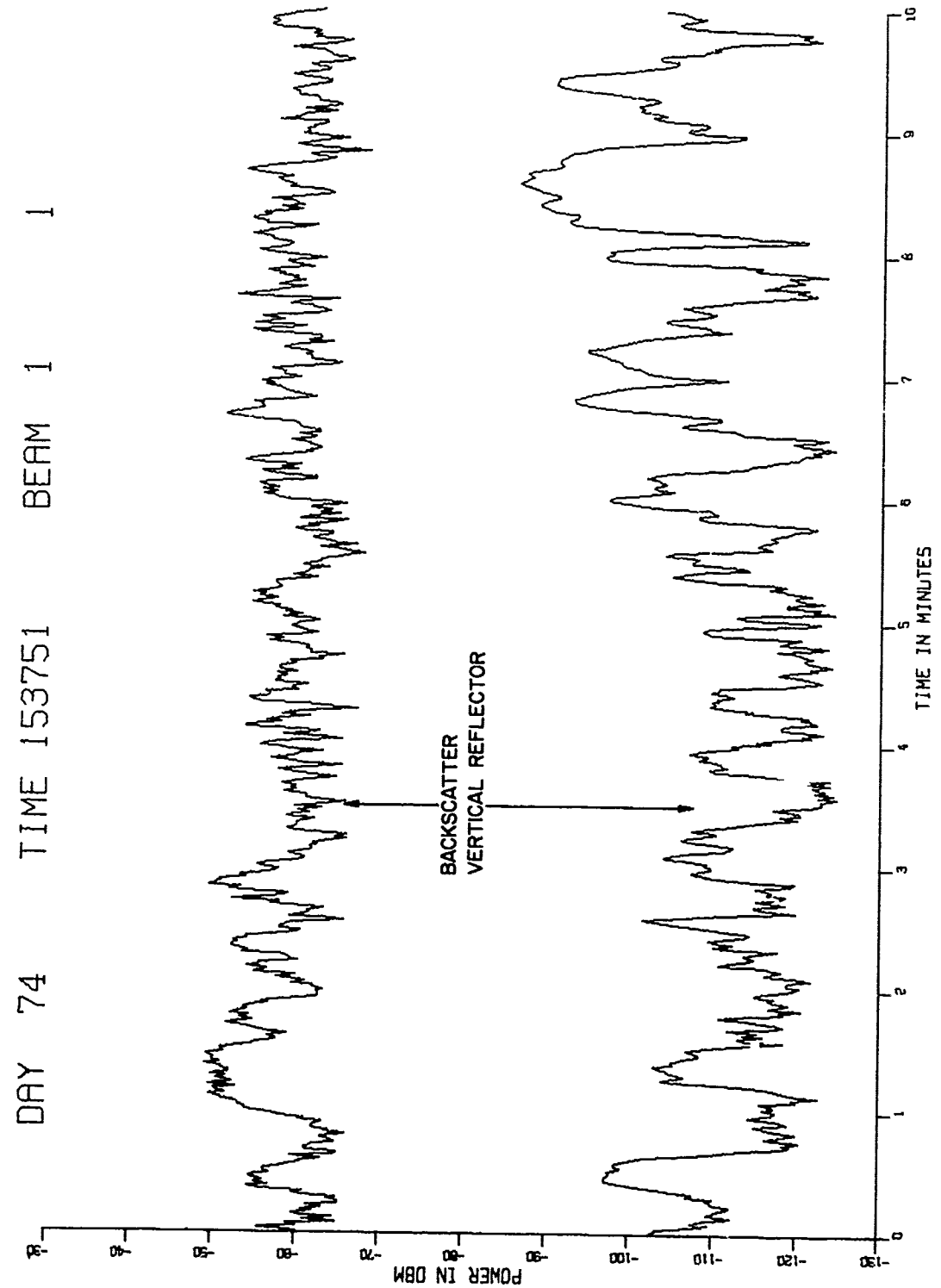

(U) Fig. 25a - Beam 1 at 1537 GMT

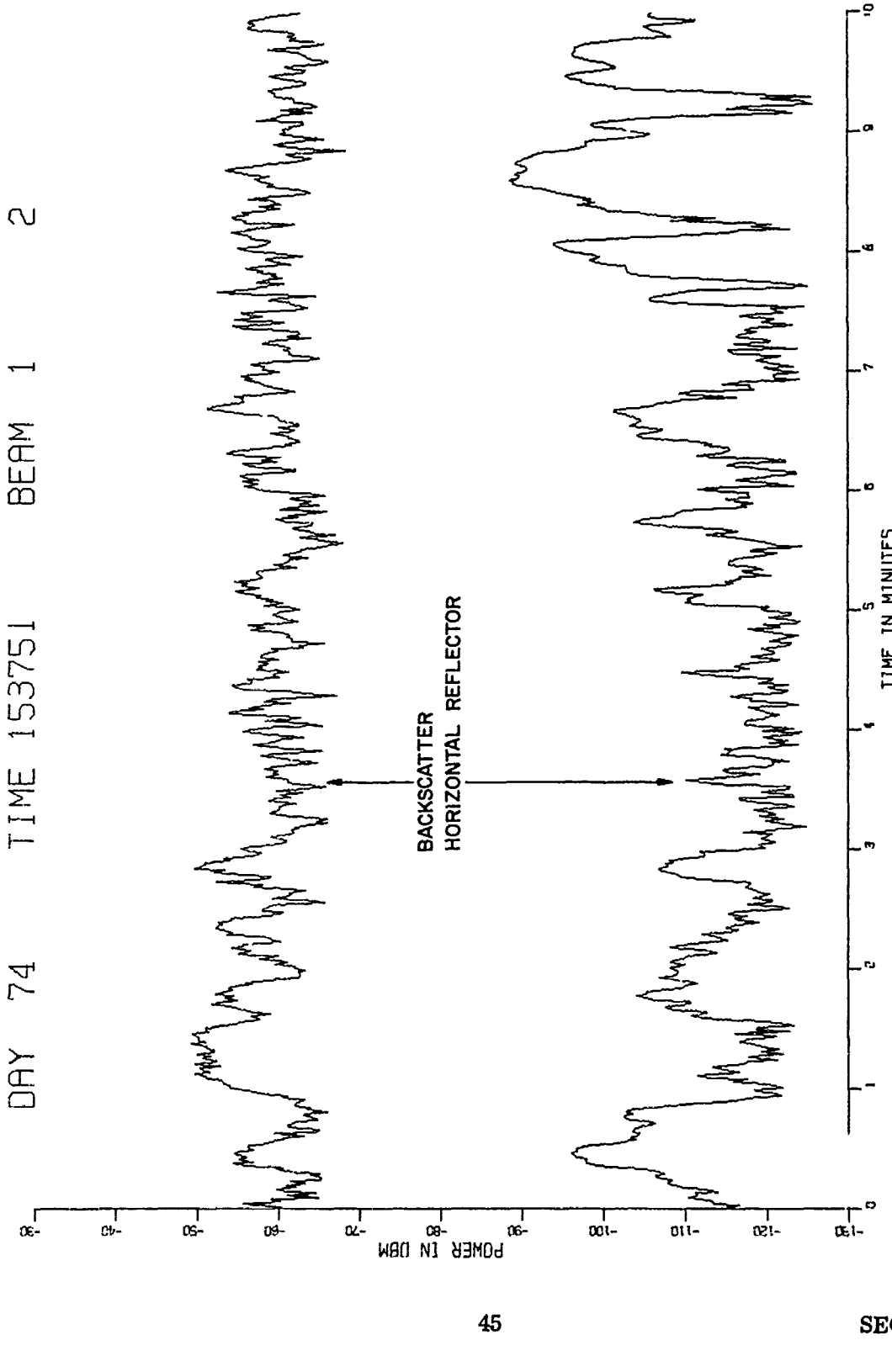

(U) Fig. 25b - Beam 1 at 1537 GMT

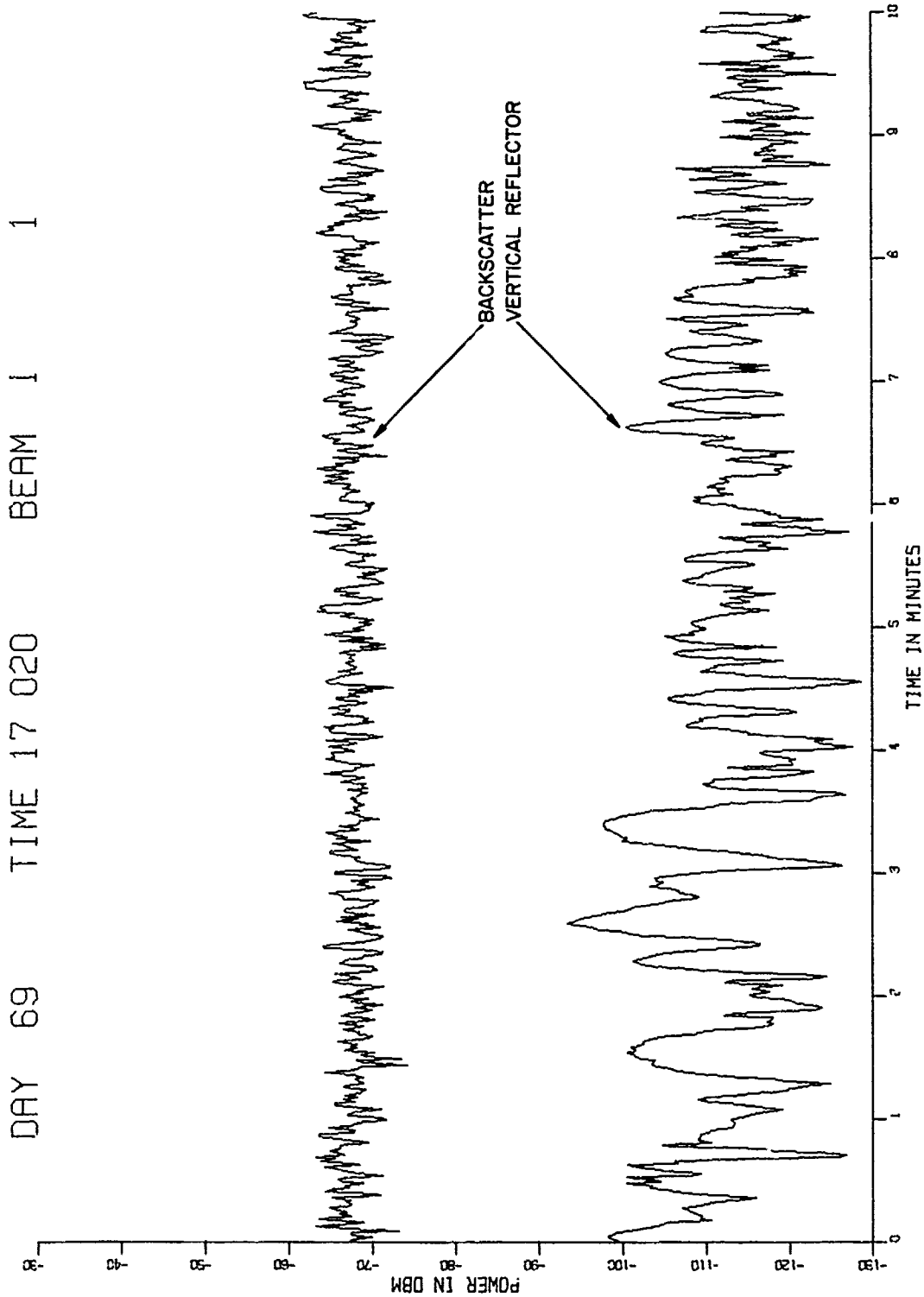

(U) Fig. 26a - Beam 1 at 1700 GMT

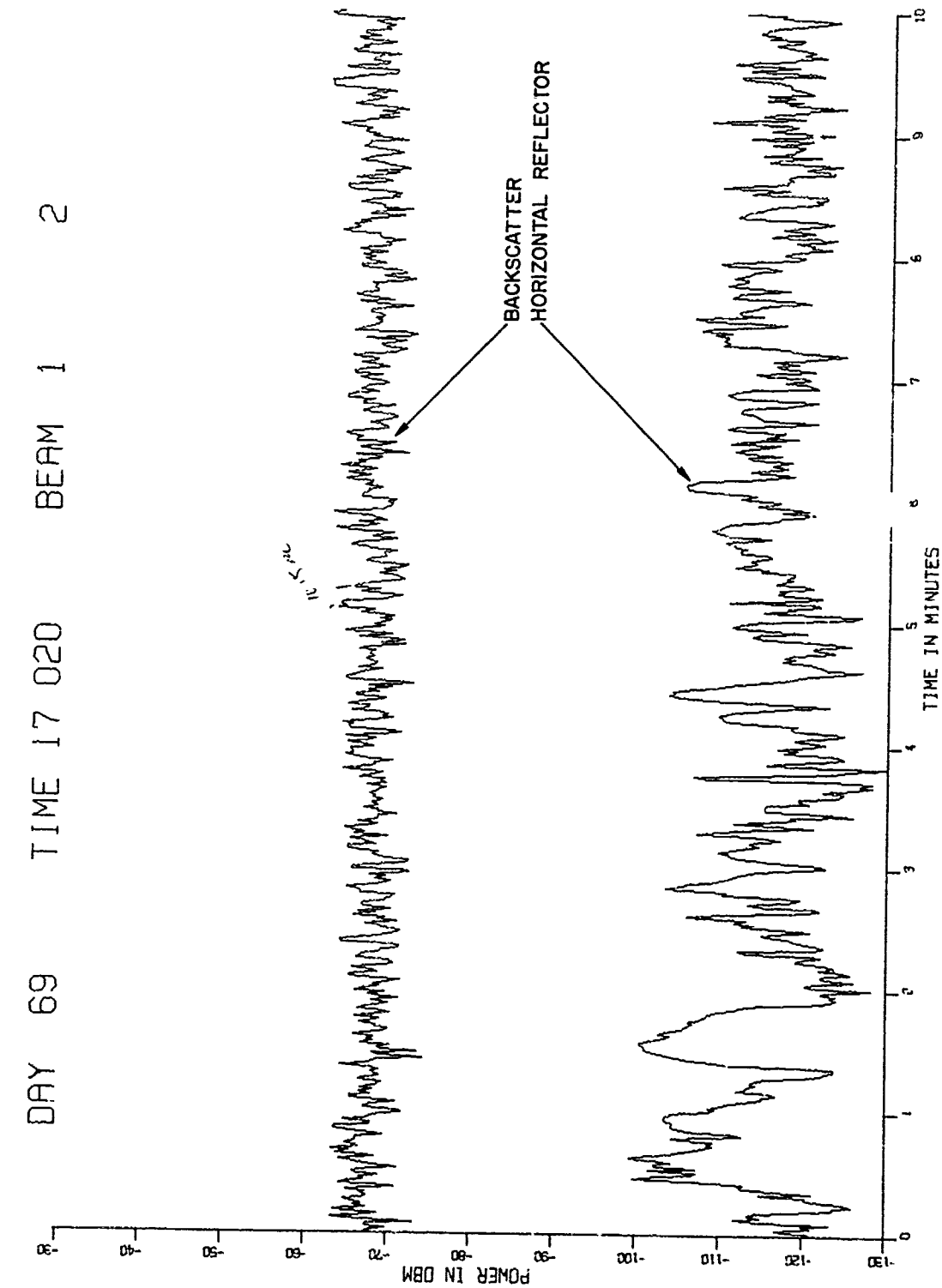

(U) Fig. 26b - Beam 1 at 1700 GMT

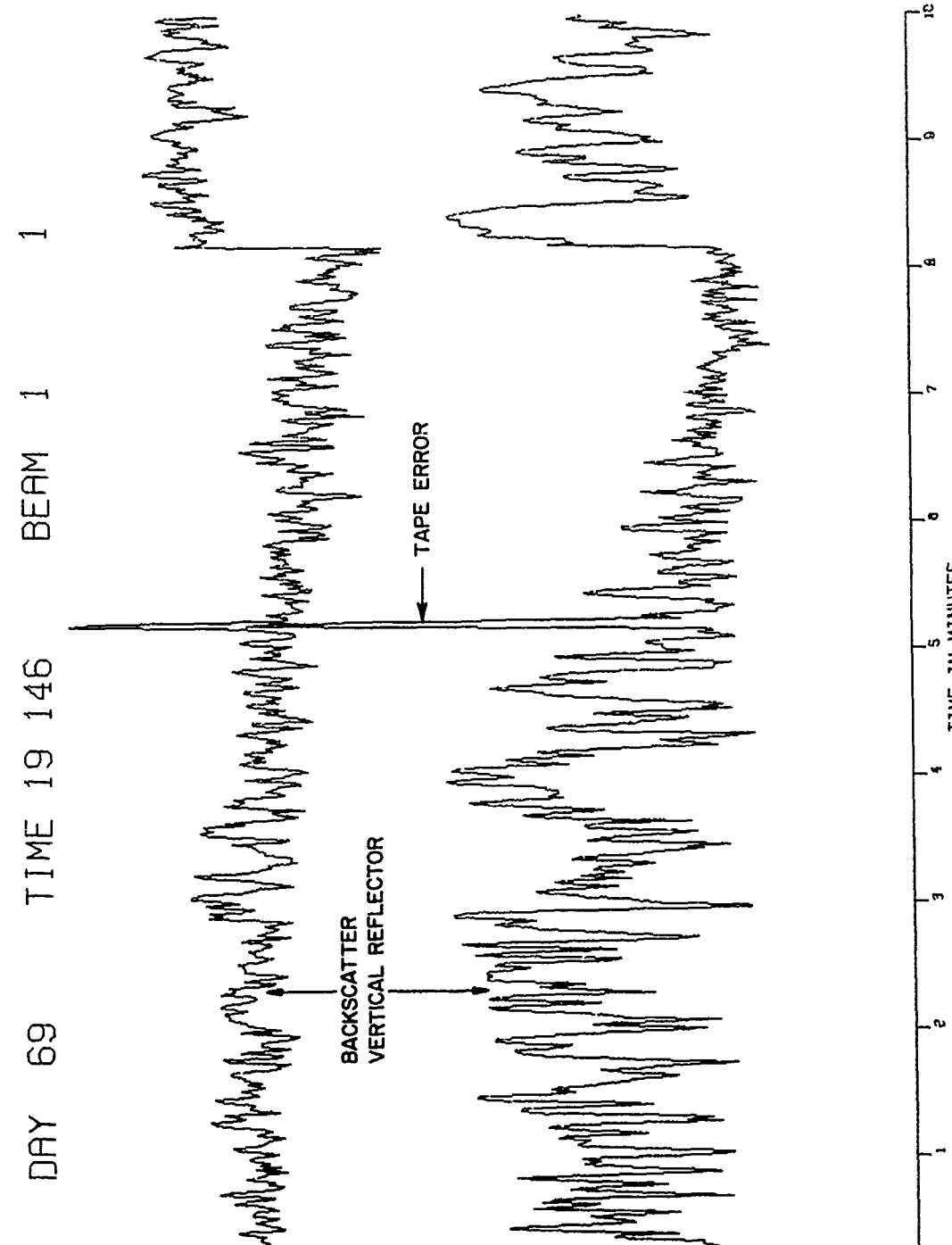

(U) Fig. 2' ı – Beam 1 at 1901 GMT

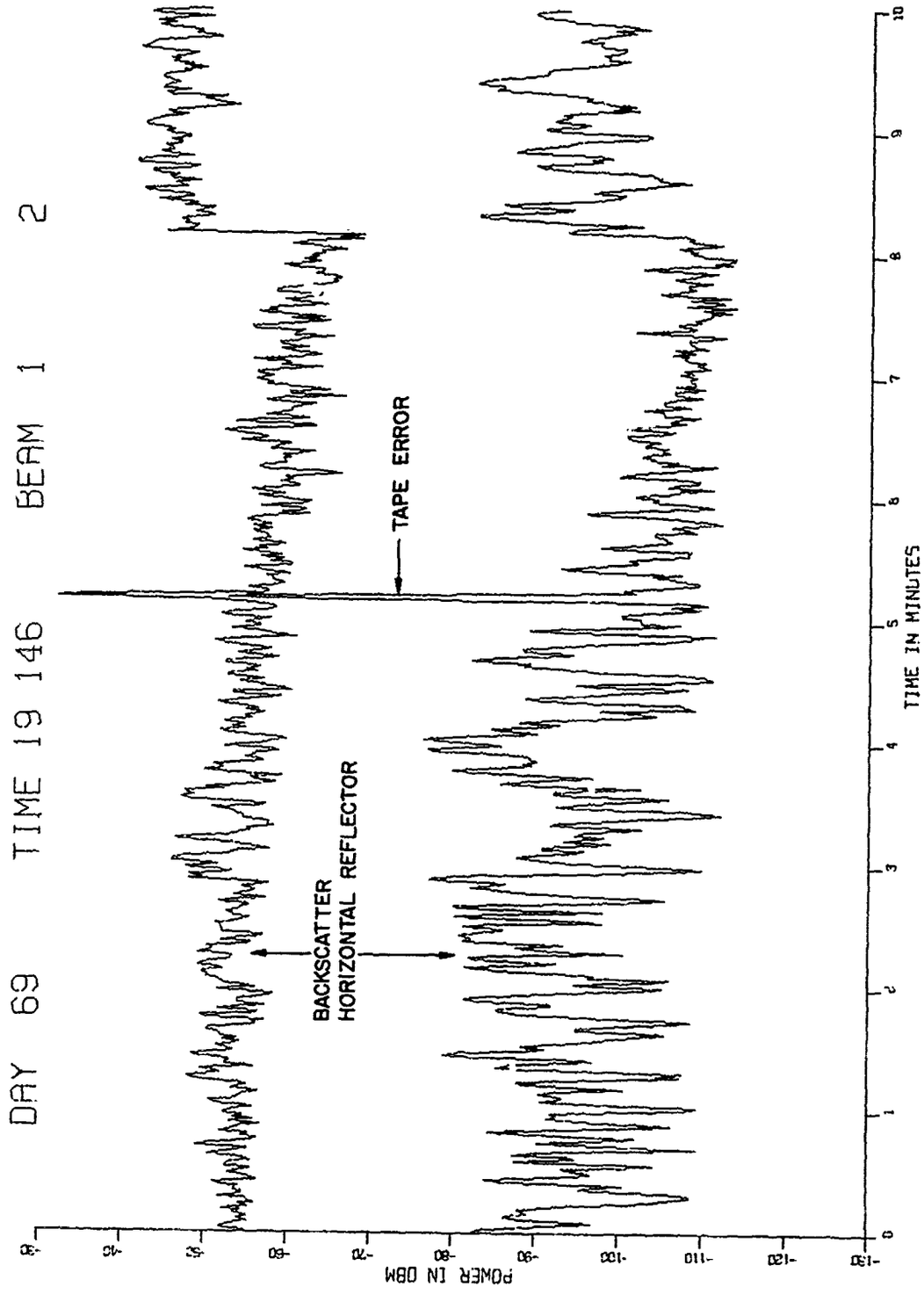

(U) Fig. 27b - Beam 1 at 1901 GMT

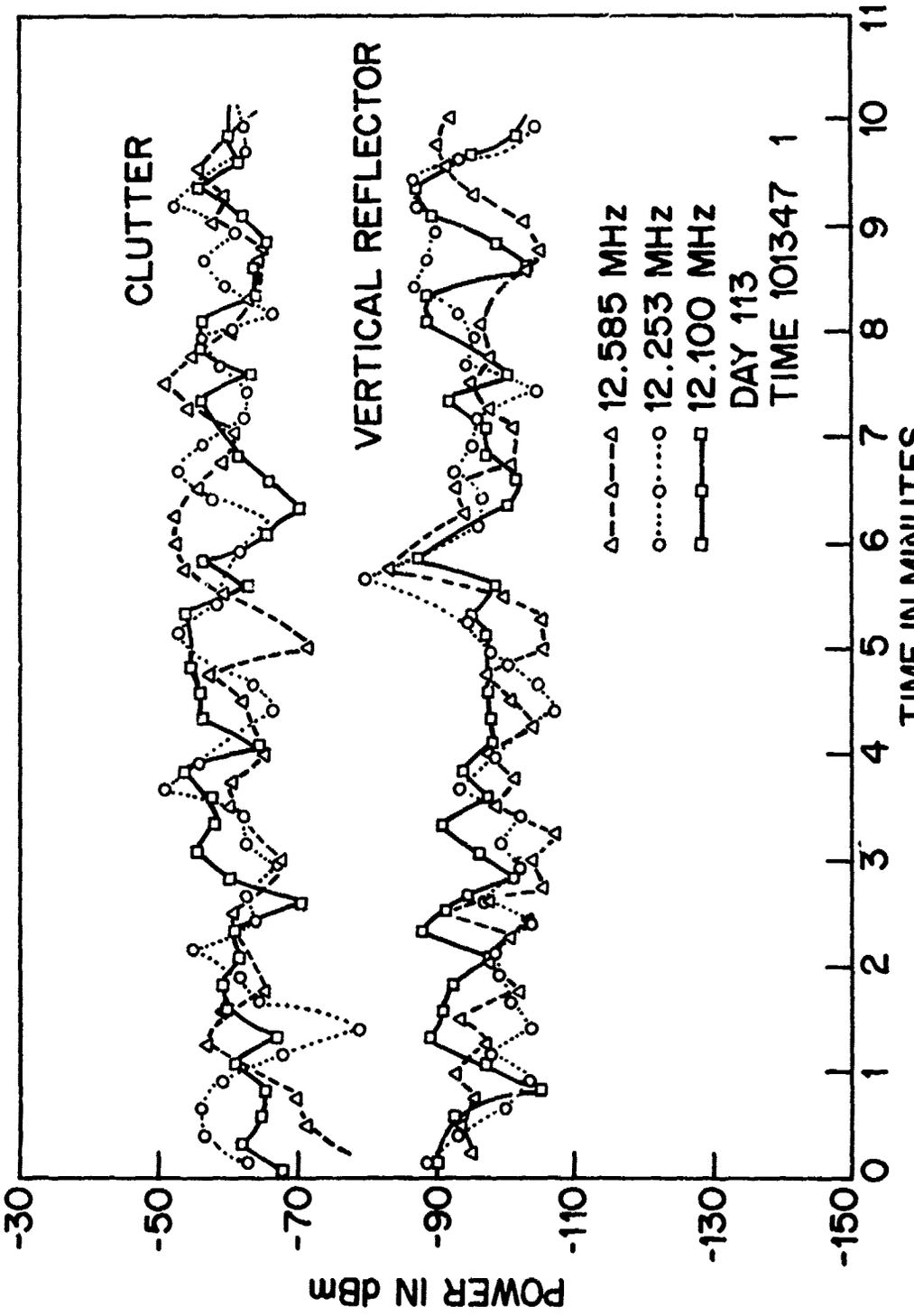

(S) Fig. 28 - Beam 2 frequency diversity clutter and vertical reflector

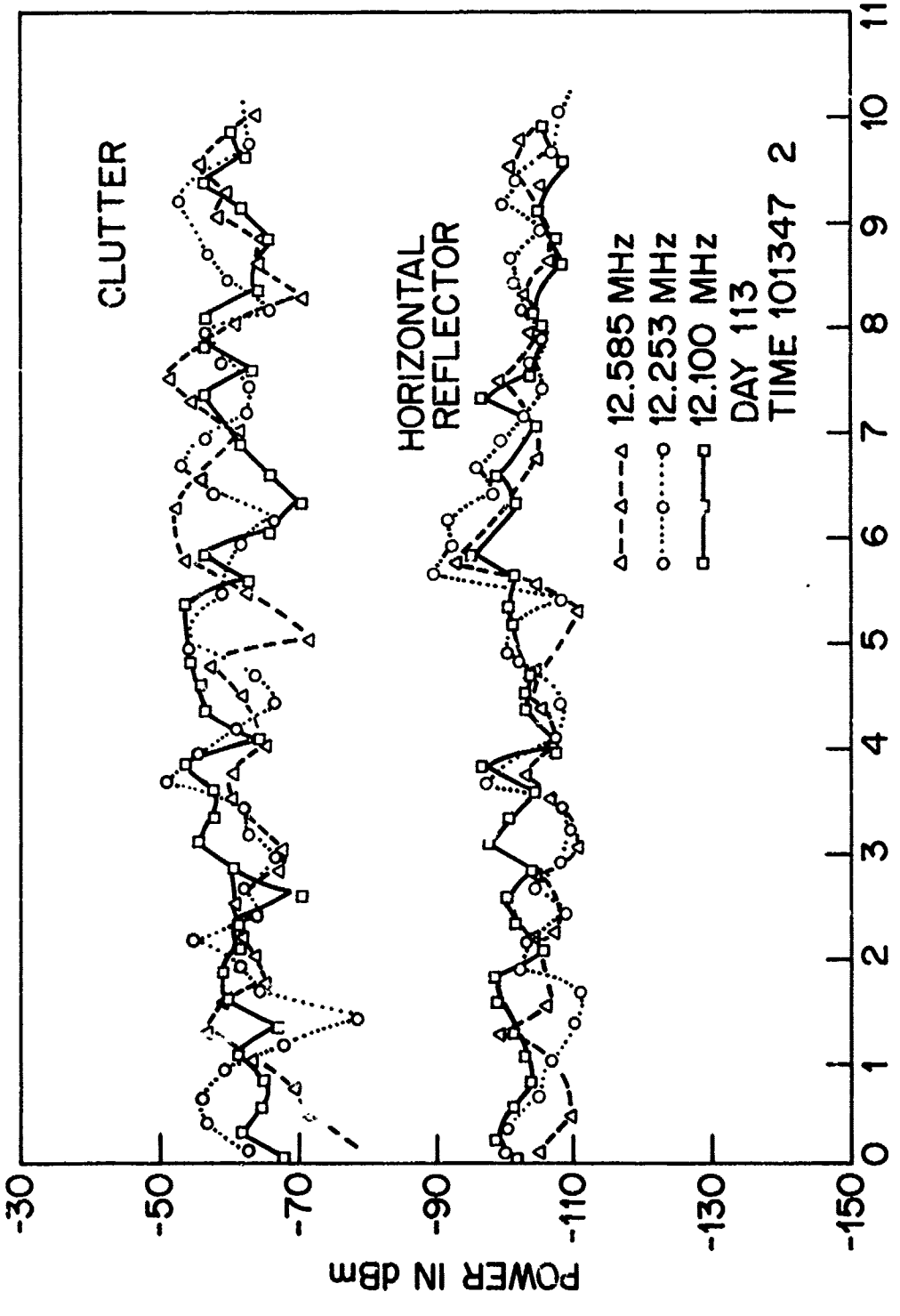

(S) Fig. 29 - Beam 2 frequency diversity clutter and horizontal reflector

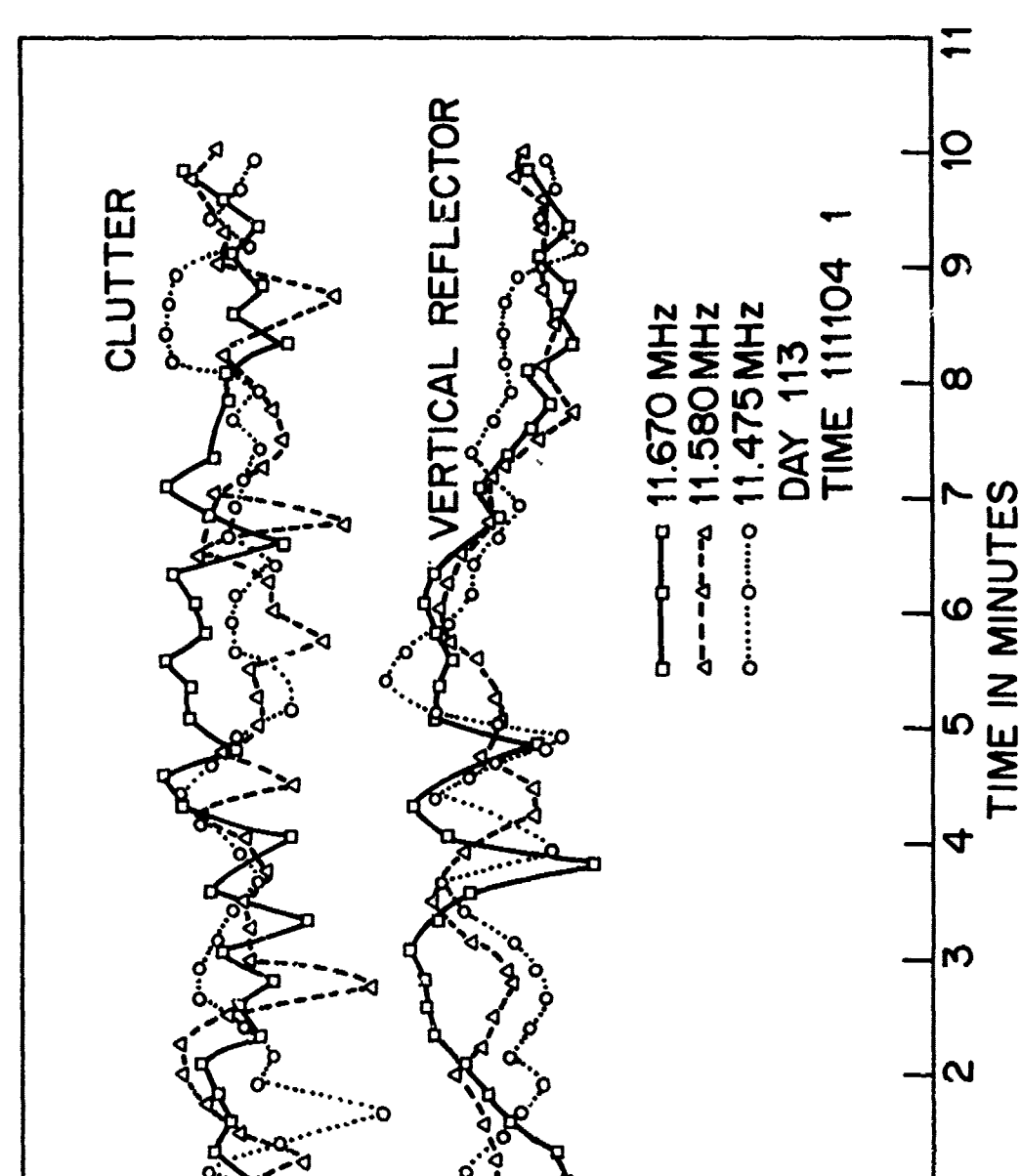

(b) Fig. 30 - Beam 4 frequency diversity clutter and vertical reflector

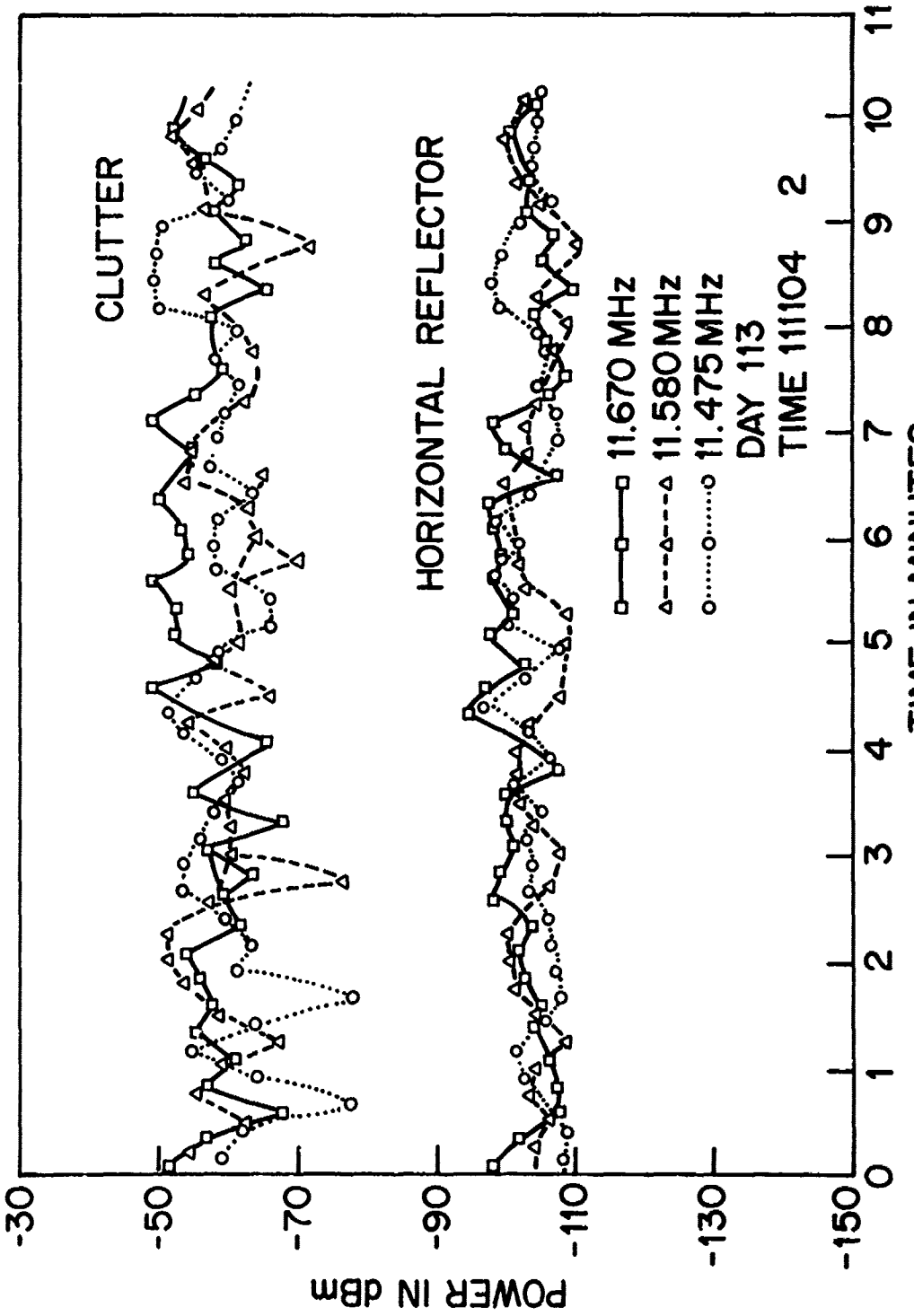

(S) Fig. 31 - Beam 2 frequency diversity clutter and horizontal reflector

MEMORANDUM

20 February 1997

Subj: Document Declassification

Ref: (1) Code 5309 Memorandum of 29 Jan. 1997
(2) Distribution Statements for Technical Publications NRL/PU/5230-95-293

Encl: (a) Code 5309 Memorandum of 29 Jan. 1997
(b) List of old Code 5320 Reports
(c) List of old Code 5320 Memorandum Reports

1. In Enclosure (a) it was recommended that the following reports be declassified, four reports have been added to the original list:

Formal: 5589, 5811, 5824, 5825, 5849, 5862, 5875, 5881, 5903, 5962, 6015, 6079, 6148, 6198, 6272, 6371, 6476, 6479, 6485, 6507, 6508, 6568, 6590, 6611, 6731, 6866, 7044, 7051, 7059, 7350, 7428, 7500, 7638, 7655. Add 7684, 7692.

Memo: 1251, 1287, 1316, 1422, [redacted], 1500, 1527, 1537, 1540, 1567, 1637, 1647, 1727, 1758, 1787, 1789, 1790, 1811, 1817, 1823, 1885, 1939, 1981, 2135, 2624, 2701, 2645, 2721, 2722, 2723, 2766. Add 2265, 2715.

The recommended distribution statement for the these reports is: **Approved for public release; distribution is unlimited.**

2. The above reports are included in the listings of enclosures (b) and (c) and were selected because of familiarity with the contents. The rest of these documents very likely should receive the same treatment.

J. M. Headrick
Code 5309

Copy:
Code 1221 — OK 2/19/97
Code 5300
Code 5320
Code 5324